

## REPORT No. 889

# VOLTERRA'S SOLUTION OF THE WAVE EQUATION AS APPLIED TO THREE-DIMENSIONAL SUPERSONIC AIRFOIL PROBLEMS

By MAX. A. HEASLET, HARVARD LOMAX, and ARTHUR L. JONES

### SUMMARY

A surface integral is developed which yields solutions of the linearized partial differential equation for supersonic flow. These solutions satisfy boundary conditions arising in wing theory. Particular applications of this general method are made, using acceleration potentials, to flat surfaces and to uniformly loaded lifting surfaces. Rectangular and trapezoidal plan forms are considered along with triangular forms adaptable to swept-forward and swept-back wings. The case of the triangular plan form in sideslip is also included. Emphasis is placed on the systematic application of the method to the lifting surfaces considered and on the possibility of further application.

### INTRODUCTION

The increased emphasis on extending theoretical knowledge in supersonic wing analysis has led to a systematic investigation of the various mathematical methods available for treating the basic differential equations. In the present report advantage has been taken of the direct analogy which exists between the linearized partial differential equation for supersonic flow in three dimensions and the two-dimensional wave equation of mathematical physics. As a result of this correspondence, solutions which have been given for the wave equation are shown to be applicable to the type of boundary condition encountered in wing problems. The first section of the report is devoted to the development of the solution for the potential of the supersonic flow field. The application of this expression to a number of examples in supersonic lifting-surface theory illustrates the usefulness of such a method of attack. In the first of these examples the loadings over the given plan forms are assumed to be uniform. The results obtained for such cases appear at first to be somewhat academic since undesirable twist and camber occur over portions of the resultant surfaces. From the uniformly loaded surfaces, however, it is possible to develop surfaces having arbitrary load distributions. Imposing the condition that the final lifting surface shall be a flat plate leads to the solution of an integral equation in every case considered. The results obtained, for some of the plan forms considered, have been developed elsewhere but not always with the unification of method attained here. New configurations are also included among the examples given. The methods shown are applicable to a large class of unsolved problems of immediate interest.

### LIST OF IMPORTANT SYMBOLS

$a$	local velocity of sound
$A$	aspect ratio $\left(\frac{b^2}{S_0}\right)$
$b$	span of wing
$c$	chord of wing
$C_L$	lift coefficient $\left(\frac{L}{qS_0}\right)$
$C(\theta)$	load distribution function
$C_0$	constant value of discontinuity in $\varphi$ over uniformly loaded lifting surface
$E(u, k)$	incomplete elliptic integral of second kind with argument $u$ and modulus $k$
$E, E'$	complete elliptic integrals of second kind with modulus $k$ and $\sqrt{1-k^2}$ , respectively
$F(u, k)$	incomplete elliptic integral of first kind with argument $u$ and modulus $k$
$H_1, H_2$	functions introduced in equations (89) and (90)
$K, K'$	complete elliptic integrals of first kind with modulus $k$ and $\sqrt{1-k^2}$ , respectively
$L$	lift of wing
$M_0$	free-stream Mach number
$n_1, n_2, n_3$	direction cosines of normals to surface $S$
$p_l$	static pressure on lower side of lifting surface
$p_u$	static pressure on upper side of lifting surface
$P: (X, Y, Z)$	point at which value of $\Omega$ is to be determined
$q$	free-stream dynamic pressure $\left(\frac{1}{2} \rho_0 V_0^2\right)$
$S$	surface enclosing volume $V$
$S_0$	area of wing
$u, v, w$	perturbation velocities in direction of $X, Y$ , and $Z$ axes, respectively
$V$	volume
$V_0$	free-stream velocity
$x, y, z$	Cartesian coordinates
$X, Y, Z$	transformed coordinates (See equation (3).)
$cn(u, k)$ $dn(u, k)$ $sn(u, k)$	Jacobi's elliptic functions of argument $u$ and modulus $k$
$\alpha$	angle of attack, radians
$\beta$	$\sqrt{M_0^2 - 1}$
$\Gamma$	Mach forecone from point $P: (X, Y, Z)$
$\Delta$	semivertex angle of triangular wing

$\Delta p$	pressure differential ( $p_i - p_u$ )
$\delta$	angle measured from $X$ axis
$\eta$	conical flow coordinate (See equations (27) and (30).)
$\theta$	$\beta \tan \delta$
$\Theta(u)$	Jacobi's theta function
$\kappa$	cylinder of infinitesimal radius enclosing axis of forecone $\Gamma$
$\lambda$	surface at which stream enters induced field of wing
$\Lambda$	angle of sideslip
$\mu$	Mach angle of the free stream ( $\mu = \arcsin \frac{1}{M_0}$ )
$\nu_1, \nu_2, \nu_3$	direction cosines of conormal $\nu$ to surface $S$
$\Pi(u, \gamma)$	incomplete elliptic integral of third kind with argument $u$ , parameter $\gamma$ , and modulus $k$
$\rho_0$	density in the free stream
$\sigma, \Omega$	variables representing either the acceleration potential, the velocity potential, or any of the three perturbation velocity components
$\tau$	surface on which boundary conditions are given
$\Phi$	velocity potential
$\varphi$	acceleration potential
$\varphi_u$	value of acceleration potential on upper side of lifting surface
$\varphi_l$	value of acceleration potential on lower side of lifting surface
$\omega$	$1 - \frac{c}{x}$

## THEORY

### LINEARIZATION OF DIFFERENTIAL EQUATION FOR COMPRESSIBLE FLOW

The quasi-linear (i. e., linear in the derivatives of highest order) differential equation for the velocity-potential  $\Phi$  in the case of compressible fluid flow in three dimensions, is expressible in the form

$$\Phi_{xx} \left(1 - \frac{\Phi_x^2}{a^2}\right) + \Phi_{yy} \left(1 - \frac{\Phi_y^2}{a^2}\right) + \Phi_{zz} \left(1 - \frac{\Phi_z^2}{a^2}\right) - 2\Phi_{yz} \frac{\Phi_y \Phi_z}{a^2} - 2\Phi_{zx} \frac{\Phi_z \Phi_x}{a^2} - 2\Phi_{xy} \frac{\Phi_x \Phi_y}{a^2} = 0 \quad (1)$$

where  $a$  represents the local velocity of sound in the medium and Cartesian coordinates are used. Under the assumptions of small perturbation theory (references 1 and 2), this equation is modified so that it is linear in form and consequently more amenable to mathematical analysis. Denoting by the variable  $\Omega$  either the acceleration potential, the velocity potential, or any of the three perturbation velocity components, the linearized expression for equation (1) is

$$(1 - M_0^2)\Omega_{xx} + \Omega_{yy} + \Omega_{zz} = 0 \quad (2)$$

where  $M_0$  is the Mach number of the free stream and thus equal to the ratio of free-stream velocity and the corresponding speed of sound.

By means of the affine transformation

$$\left. \begin{aligned} X &= x \\ Y &= \sqrt{\pm(1 - M_0^2)} y \\ Z &= \sqrt{\pm(1 - M_0^2)} z \end{aligned} \right\} \quad (3)$$

equation (2) can be put into standard forms. Thus, when  $M_0 < 1$  the plus signs are chosen in the radicals of equation (3) and equation (2) becomes

$$\Omega_{xx} + \Omega_{yy} + \Omega_{zz} = 0 \quad (4)$$

while for  $M_0 > 1$  the minus signs are used and, as a consequence,

$$\Omega_{xx} - \Omega_{yy} - \Omega_{zz} = 0 \quad (5)$$

For the case of subsonic flow ( $M_0 < 1$ ) the linearized equation is thereby reduced to the well-known Laplace equation in three dimensions. Similarly, in supersonic flow ( $M_0 > 1$ ) equation (2) is again reduced to classical type with the replacement of the space coordinate  $X$  by a time variable  $T$  to give the two-dimensional wave equation of mathematical physics. The linearization of the general differential equation for compressible fluid flow therefore makes available, in both subsonic and supersonic studies, the results of the extensive work carried out in previous research on problems related to equations (4) and (5).

### APPLICATION OF GREEN'S THEOREM TO LINEARIZED COMPRESSIBLE FLOW EQUATION

Methods of solution for partial differential equations of the type considered here may be classified into two principal categories: methods which express the solutions in terms of orthogonal functions and methods which are based on the use of Green's theorem. Volterra's solution, discussions of which may be found in references 3, 4, and 5, applies the latter approach to the two-dimensional wave equation and, as a consequence, his results may be adapted to the study of supersonic flow and specific solutions of equation (5).

If the functional notation

$$L(\Omega) \equiv \Omega_{xx} - \Omega_{yy} - \Omega_{zz}$$

is used, the analytic form of Green's theorem for equation (5), relating a volume integral over the region  $V$  to a surface integral over the surface  $S$  enclosing  $V$ , may be written in the form

$$\iiint_V [\sigma L(\Omega) - \Omega L(\sigma)] dV = - \iint_S (\sigma D_n \Omega - \Omega D_n \sigma) dS$$

where  $\sigma, \Omega$  are any two functions which, together with their first and second derivatives, are finite and single valued throughout the region considered, and

$$D_n \Omega = n_1 \frac{\partial \Omega}{\partial X} - n_2 \frac{\partial \Omega}{\partial Y} - n_3 \frac{\partial \Omega}{\partial Z}$$

where  $n_1, n_2, n_3$  are direction cosines of inward normals to the surface  $S$ .

The expression for  $D_n \Omega$  is, of course, a directional derivative. The corresponding term appearing in Green's theorem

for Laplace's differential equation (incompressible fluid flow) is precisely the directional derivative along the normal to the surface  $S$ . The analogy between the two terms prompts the introduction of the so-called conormal to  $S$  with direction cosines  $\nu_1, \nu_2, \nu_3$  defined as

$$\nu_1 = -n_1, \nu_2 = n_2, \nu_3 = n_3$$

The geometrical connection between the normal and the conormal is indicated in figure 1; the angles between the lines and the  $Y$  and  $Z$  axes remain respectively equal, while the angles between the lines and the  $X$  axis are supplementary.

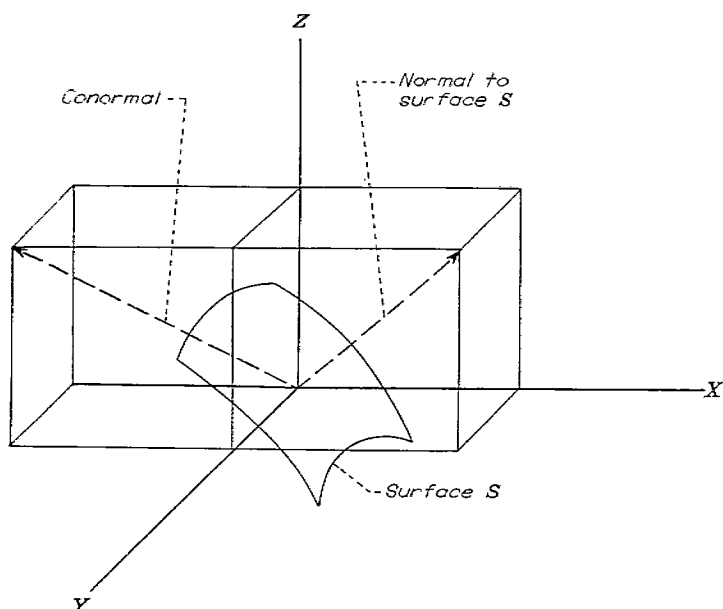


FIGURE 1.—The geometric relations between normal and conormal to surface  $S$ .

It follows, in particular, that if the surface  $S$  is the  $XY$  plane the two lines are coincident; if  $S$  is a cone with semivertex angle equal to  $45^\circ$  and axis parallel to the  $X$  axis, the conormal at any point lies long the surface  $S$ .

It is now possible to write

$$-D_n \Omega = \nu_1 \frac{\partial \Omega}{\partial X} + \nu_2 \frac{\partial \Omega}{\partial Y} + \nu_3 \frac{\partial \Omega}{\partial Z} = \frac{\partial \Omega}{\partial \nu} \quad (6)$$

and the surface-volume relation becomes

$$\iiint_V [\sigma L(\Omega) - \Omega L(\sigma)] dV = \iint_S \left[ \sigma \frac{\partial \Omega}{\partial \nu} - \Omega \frac{\partial \sigma}{\partial \nu} \right] dS \quad (7)$$

If  $\Omega$  and  $\sigma$  are chosen so as to satisfy equation (5) throughout the region  $V$ , then equation (7) reduces to the form

$$\iint_S \sigma \frac{\partial \Omega}{\partial \nu} dS = \iint_S \Omega \frac{\partial \sigma}{\partial \nu} dS \quad (8)$$

The form of equation (8) is a direct analogue to results obtainable for functions satisfying Laplace's equation. (See, e. g., reference 6, p. 46.) The use of the conormal produces this symbolic equivalence.

#### VOLTERRA'S METHOD FOR TWO-DIMENSIONAL WAVE EQUATION

Consider now a surface  $\tau$  which, for the purposes of this report, may be thought of as being coincident with the  $XY$  plane and parallel to the air flow which is in the direction of the positive  $X$  axis. Two such surfaces are represented by the darkened areas in figures 2(a) and 2(b). It is desired to determine the value of  $\Omega$  at the point  $P(X, Y, Z)$  from a knowledge of the boundary conditions given on  $\tau$ . The solution to such a problem is immediately suggested by equation (8) since that equation requires only the knowledge of  $\Omega$  and  $\frac{\partial \Omega}{\partial \nu}$  along a surface enclosing a given volume, together

with the knowledge of some particular solution  $\sigma$  to the wave equation valid everywhere within the enclosed volume. Further, it is physically evident that contributions to the value of  $\Omega$  at  $P$  can come only from points within the forecone with vertex at  $P$  and also within the envelope of the aftercones with vertices at the foremost disturbance points of  $\tau$ . Referring to figure 2(a), this would mean the volume bounded by the forecone  $\Gamma$  and the wedge  $\lambda$  springing from the leading edge of  $\tau$ ; and in figure 2(b), the volume bounded by the forecone  $\Gamma$  and the aftercone  $\lambda$  with vertex at the apex of the surface  $\tau$ . Since for the boundary-value problems involved the surface  $\tau$  remains in the  $XY$  plane, equation (8) must be applied to all three surfaces  $\lambda, \Gamma$ , and  $\tau$ .

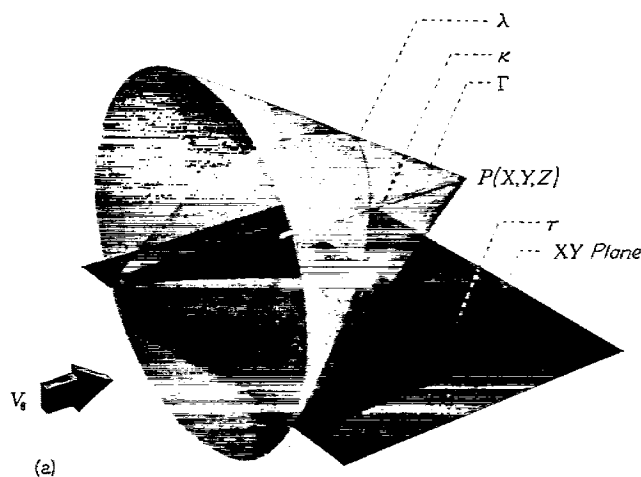


FIGURE 2.—Mach forecone from point  $P(X, Y, Z)$  intersecting surface  $\tau$ . (a) Rectangular plan form.

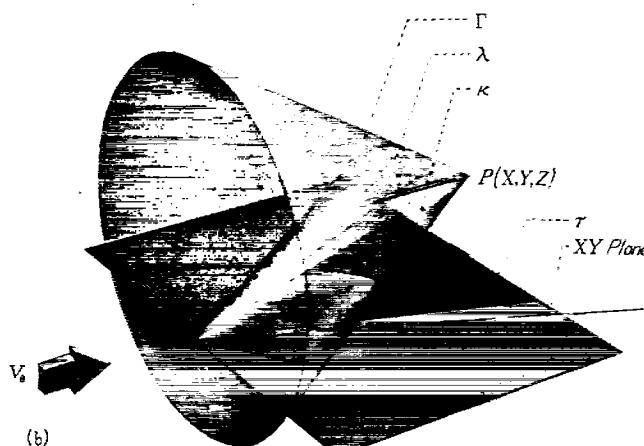


FIGURE 2.—Concluded. (b) Triangular plan form.

Since there is no way of determining  $\Omega$  and  $\frac{\partial \Omega}{\partial \nu}$  along  $\Gamma$  the attempted solution will be especially difficult unless the particular solution  $\sigma$  and its derivative with respect to the conormal vanish everywhere on  $\Gamma$ . But this is in fact the essential part of Volterra's method of solution. Thus the proper choice of  $\sigma$  is

$$\sigma = \text{arc cosh} \frac{X - X_1}{\sqrt{(Y - Y_1)^2 + (Z - Z_1)^2}}$$

(This relation, incidentally, is the indefinite integral of the fundamental solution representing a supersonic source in three dimensions  $[(X - X_1)^2 - (Y - Y_1)^2 - (Z - Z_1)^2]^{-1/2}$ .) The value of  $\sigma$  is equal to zero on the forecone  $\Gamma$  since the equation of this cone is

$$(X - X_1)^2 - (Y - Y_1)^2 - (Z - Z_1)^2 = 0$$

and further, since the conormal is always directed along the forecone,  $\frac{\partial \sigma}{\partial \nu}$  is the gradient of  $\sigma$  along  $\Gamma$  and is also zero.

Equation (8) provides an equality for the distribution of  $\Omega$  and  $\frac{\partial \Omega}{\partial \nu}$  over  $\lambda$  and  $\tau$ , provided  $\Omega$  and  $\sigma$  satisfy equation (5) throughout the enclosed volume mentioned. However, although  $\sigma$  satisfies equation (5) everywhere in the enclosed volume opposite  $\tau$  from  $P$  (under the  $XY$  plane in fig. 2), along the line  $(Y - Y_1)^2 + (Z - Z_1)^2 = 0$  (above the  $XY$  plane in fig. 2)  $\sigma$  is infinite and does not satisfy the assumptions made in establishing Green's theorem. If this line is excluded, however, by means of a cylinder  $\kappa$  of radius  $\epsilon$ , with axis lying along the line  $(Y - Y_1)^2 + (Z - Z_1)^2 = 0$ , then equation (8) may be applied to the region outside  $\kappa$  and yet within the space bounded by  $\lambda$ ,  $\tau$ , and  $\Gamma$ . In fact equation (8) can then be written

$$\int \int_{\tau + \kappa + \lambda} \left( \Omega \frac{\partial \sigma}{\partial \nu} - \sigma \frac{\partial \Omega}{\partial \nu} \right) dS = 0 \quad (9)$$

where  $\tau_1$  is the portion of  $\tau$  bounding the region of integration. If  $R = \sqrt{(Y - Y_1)^2 + (Z - Z_1)^2}$  and cylindrical coordinates  $\epsilon$ ,  $\psi$ , and  $(X - X_1)$  are used, an element of area on the cylinder  $\kappa$  is  $dS = -\epsilon d\psi d(X - X_1)$ , while

$$\frac{\partial \sigma}{\partial \nu} = \frac{\partial \sigma}{\partial R} = -\frac{(X - X_1)}{\epsilon \sqrt{(X - X_1)^2 - \epsilon^2}}$$

so that

$$\begin{aligned} \lim_{\epsilon \rightarrow 0} \int \int_{\kappa} \left( \Omega \frac{\partial \sigma}{\partial \nu} - \sigma \frac{\partial \Omega}{\partial \nu} \right) dS &= \lim_{\epsilon \rightarrow 0} \int \int_{\kappa} \frac{\epsilon \Omega (X - X_1) d\psi d(X - X_1)}{\epsilon \sqrt{(X - X_1)^2 - \epsilon^2}} \\ \lim_{\epsilon \rightarrow 0} \int \int_{\kappa} \epsilon \frac{\partial \Omega}{\partial \nu} \text{arc cosh} \left( \frac{X - X_1}{\epsilon} \right) d\psi d(X - X_1) &= \\ \int \int_{\kappa} -\Omega d\psi dX_1 - \int \int_{\kappa} \lim_{\epsilon \rightarrow 0} \frac{\partial \Omega}{\partial \nu} \left( \ln \frac{X_1 - X}{\epsilon} \right) \epsilon d\psi d(X - X_1) &= \\ = -2\pi \int_{X_1}^X \Omega(\xi, Y, Z) d\xi \end{aligned} \quad (10)$$

If this result is applied to equation (9), one gets

$$2\pi \int_{X_1}^X \Omega(\xi, Y, Z) d\xi = \int \int_{\tau + \lambda} \left( \Omega \frac{\partial \sigma}{\partial \nu} - \sigma \frac{\partial \Omega}{\partial \nu} \right) dS \quad (11)$$

and, after differentiating equation (11) with respect to  $X$ ,

$$\Omega(X, Y, Z) = \frac{1}{2\pi} \frac{\partial}{\partial X} \int \int_{\tau + \lambda} \left( \Omega \frac{\partial \sigma}{\partial \nu} - \sigma \frac{\partial \Omega}{\partial \nu} \right) dS \quad (12)$$

#### PROCEDURE FOR LIFTING SURFACES AND SYMMETRIC WINGS

When the region considered is that bounded by the surface  $\tau$ ,  $\Gamma$ , and  $\lambda'$ , the portion of  $\lambda$  on the opposite side of  $\tau$  from the point  $P$ , then  $\sigma$  is finite throughout the region and, as a direct consequence of equation (9),

$$0 = -\frac{1}{2\pi} \frac{\partial}{\partial X} \int \int_{\tau + \lambda'} \left( \Omega' \frac{\partial \sigma}{\partial \nu'} - \sigma \frac{\partial \Omega'}{\partial \nu'} \right) dS \quad (13)$$

where  $\Omega'$  is the value of the potential function on the side of  $\tau$  opposite  $P$  and  $\nu'$  is in the opposite direction to  $\nu$  on  $\tau$ . Adding equations (12) and (13),

$$\begin{aligned} \Omega(X, Y, Z) &= \frac{-1}{2\pi} \frac{\partial}{\partial X} \int \int_{\tau_1} \left( \frac{\partial \Omega}{\partial \nu} + \frac{\partial \Omega'}{\partial \nu'} \right) \sigma dS + \\ \frac{1}{2\pi} \frac{\partial}{\partial X} \int \int_{\tau_1} (\Omega - \Omega') \frac{\partial \sigma}{\partial \nu} dS &+ \frac{1}{2\pi} \frac{\partial}{\partial X} \int \int_{\lambda} \left( \Omega \frac{\partial \sigma}{\partial \nu} - \sigma \frac{\partial \Omega}{\partial \nu} \right) dS + \\ \frac{1}{2\pi} \frac{\partial}{\partial X} \int \int_{\lambda'} \left( \Omega' \frac{\partial \sigma}{\partial \nu'} - \sigma \frac{\partial \Omega'}{\partial \nu'} \right) dS \end{aligned}$$

The integrations over  $\tau$  are now in a form which may be interpreted directly in terms of known conditions over bodies with given load or symmetrical section. The integration over  $\lambda$  and  $\lambda'$  can be disposed of by discussing the two cases shown in figure 2. When  $\Omega$  is identified with the velocity potential, its value can be shown to be zero on  $\lambda$  and  $\lambda'$  regardless of whether the leading edge is swept ahead of or behind the Mach cone. When  $\Omega$  represents acceleration potential or any of the perturbation velocity components, a discontinuity exists in the value of  $\Omega$  for leading edges swept ahead of the Mach cone as in figure 2 (a). Analysis of this case, however, reveals that for all wing problems the integration over  $\lambda$  just cancels the integration over  $\lambda'$ . When the leading edge is swept behind the Mach cone as in figure 2 (b) the value of  $\Omega$  is again zero. Thus in any case there results the fundamental equation:

$$\begin{aligned} \Omega(X, Y, Z) &= \frac{-1}{2\pi} \frac{\partial}{\partial X} \int \int_{\tau_1} \left( \frac{\partial \Omega}{\partial \nu} + \frac{\partial \Omega'}{\partial \nu'} \right) \sigma dS + \\ \frac{1}{2\pi} \frac{\partial}{\partial X} \int \int_{\tau_1} (\Omega - \Omega') \frac{\partial \sigma}{\partial \nu} dS \end{aligned} \quad (14)$$

The counterpart of equation (14) for incompressible fluid flow is well known. (See, e. g., p. 60 reference 6.)

Under the particular conditions for which

$$\frac{\partial \Omega}{\partial \nu} = -\frac{\partial \Omega'}{\partial \nu'} \quad (15)$$



over the surface  $\tau$  equation (14) becomes

$$\Omega(X, Y, Z) = \frac{1}{2\pi} \frac{\partial}{\partial X} \int \int_{\tau_1} (\Omega - \Omega') \frac{\partial \sigma}{\partial \nu} dS \quad (16)$$

The restrictions imposed in equation (15) can be given physical significance after the functions  $\Omega$ ,  $\Omega'$ , and the surface  $\tau$  have been given specific meanings. Consider first the case where  $\tau$  is a lifting surface. Obviously the normal induced velocity  $w$  is a continuous function across  $\tau$ . If  $\Omega$  and  $\Omega'$  are velocity potentials associated with the lifting surface,

$$w(X, Y, Z) = w'(X, Y, Z) = \frac{\partial \Omega}{\partial \nu} = -\frac{\partial \Omega'}{\partial \nu'}$$

and equation (15) is satisfied. If  $\Omega$  denotes acceleration potential or perturbation velocity  $u$ , it is necessary to show that on the lifting surface

$$\frac{\partial u}{\partial \nu} = -\frac{\partial u'}{\partial \nu'}$$

This relation holds, however, for since  $w(X, Y, Z) = w'(X, Y, Z)$  along  $\tau$ , it follows that

$$\frac{\partial w}{\partial X} = \frac{\partial w'}{\partial X'}$$

and from the condition of irrotationality it is possible to express the gradient of  $w$  in the  $X$  direction as the gradient of  $u$  normal to the surface, that is, in the directions of  $\nu$  and  $\nu'$ . Equation (16) is thus applicable directly to lifting-surface theory in conjunction with either velocity or acceleration potentials. Application can also be made to the determination of pressure distribution over the surface of a symmetric airfoil at zero angle of attack. In this so-called nonlifting case the function  $\Omega$  is set equal to the induced velocity  $w$ ,  $\tau$  is the plane of symmetry of the airfoil, and equation (16) can be used to establish the boundary conditions, provided equation (15) is satisfied. For this to be so  $\partial w / \partial \nu$  must equal  $-\partial w' / \partial \nu'$ . But conditions of symmetry give  $w(Z) = -w'(-Z)$  from which the equality is seen to hold.

#### RETRANSFORMATION OF COORDINATES

Since

$$\sigma = \text{arc cosh} \frac{X - X_1}{\sqrt{(Y - Y_1)^2 + (Z - Z_1)^2}}$$

direct substitution into equation (16) yields

$$\Omega(X, Y, Z) =$$

$$\frac{1}{2\pi} \frac{\partial}{\partial X} \int \int_{\tau_1} \frac{(\Omega - \Omega')(X - X_1)(Z - Z_1) dX_1 dY_1}{[(Y - Y_1)^2 + (Z - Z_1)^2] \sqrt{(X - X_1)^2 - (Y - Y_1)^2 - (Z - Z_1)^2}}$$

This solution applies to equation (5) and, in order to relate problems to the linearized equation (2), it is necessary to use the transformation of equations (3). If the point  $X_1, Y_1, Z_1$  transforms to the point  $x_1, y_1, z_1$ , it follows that

$$\Omega(x, y, z) =$$

$$\frac{1}{2\pi} \frac{\partial}{\partial x} \int \int_{\tau_1} \frac{(\Omega - \Omega')(x - x_1)(z - z_1) dx_1 dy_1}{[(y - y_1)^2 + (z - z_1)^2] \sqrt{(x - x_1)^2 - \beta^2[(y - y_1)^2 + (z - z_1)^2]}} \quad (17)$$

where

$$\beta^2 = M_0^2 - 1$$

#### APPLICATIONS

##### GENERAL REMARKS

Applications in lifting-surface theory may proceed along two possible lines depending upon the boundary conditions specified. In what is usually referred to as the direct problem, or problem of the first kind, the loading is given over the wing and the potential function of the flow field is calculated. From the potential function the shape of the aerodynamic surface supporting this load can be found relatively easily. The inverse problem, or problem of the second kind, concerns itself with the determination of the loading over a wing surface from a knowledge of the surface shape. In the following sections both of these cases will be considered. The direct problem will be discussed for various plan forms, the analysis proceeding directly from the expression for the potential function given in equation (17). The detailed discussion of the direct problem is justified by its application to the inverse problem where the loading over flat plates with rectangular, trapezoidal, and triangular plan forms is determined. The mathematics of the inverse problem is less straightforward since the analysis involves the introduction of elemental lifting surfaces with constant loading and the solution of an integral equation for each plan form.

##### UNIFORMLY LOADED LIFTING SURFACES IN SUPERSONIC FLOW

**Infinite span wing.**—In order to determine the induced velocities on the surface of an infinite span, uniformly loaded, supersonic lifting surface by means of the methods derived in the preceding section, it is convenient to set  $\Omega$  equal to the acceleration potential  $\varphi$  (reference 2). The lifting surface is, in this case, a surface of discontinuity for the function  $\varphi$  and corresponds to the surface  $\tau_1$  in equation (17). The discontinuity in the value of  $\varphi$  between the upper and lower surface is equal to

$$(\varphi_u - \varphi_l) = \frac{1}{\rho_0} (p_l - p_u)$$

where

$\rho_0$  density in the free stream

$p_l$  static pressure on lower surface

$p_u$  static pressure on upper surface

It follows that for the uniformly loaded wing in the plane  $z_1 = 0$  the discontinuity in the acceleration potential is a constant, say  $C_0$ . From equation (17)

$$\varphi(x, y, z) = \frac{C_0}{2\pi} \frac{\partial}{\partial x} \int \int \frac{(x - x_1)z dx_1 dy_1}{[(y - y_1)^2 + z^2] \sqrt{(x - x_1)^2 - \beta^2[(y - y_1)^2 + z^2]}} \quad (18)$$

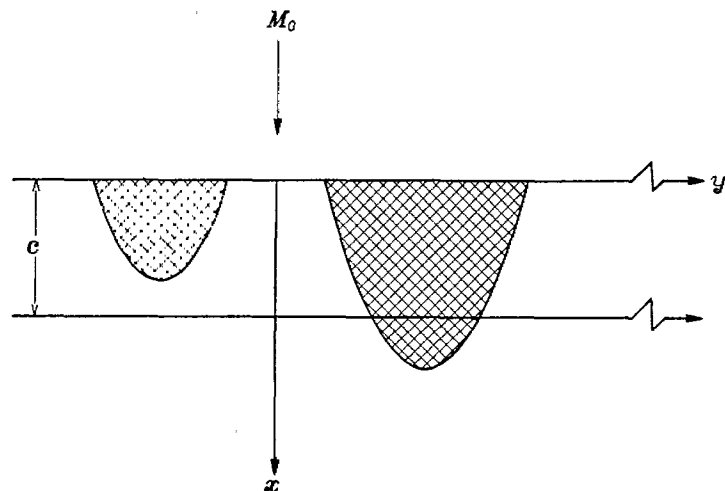


FIGURE 3.—Regions of integration for infinite span unswept wing.

A sketch of the airfoil plan form is given in figure 3 and two possible regions of integration are indicated. In all cases the integration with respect to  $y$  is performed between the limits at which the radical

$$\sqrt{(x-x_1)^2 - \beta^2[(y-y_1)^2 + z^2]}$$

vanishes while the integration with respect to  $x$  depends upon the manner in which the forecone of the point  $P$  intersects the discontinuity surface. Denoting the chord length of the airfoil by  $c$ , the following relations are obtained:

$$\begin{aligned} \varphi &= 0 \text{ when } x \mp \beta z < 0 \\ \varphi &= \pm \frac{1}{2} C_0 \text{ when } 0 \leq x \mp \beta z \leq c \\ \varphi &= 0 \text{ when } c < x \mp \beta z \end{aligned} \quad (19)$$

(When double signs are used, the upper sign refers always to the case where  $z > 0$  and the lower sign corresponds to  $z < 0$ .)

The value of the acceleration potential is thus seen to be zero at all points in space except for those points lying within the region between the wedges extending back from the leading and trailing edges of the airfoil.

It is now possible to determine the induced velocities associated with the acceleration potential just obtained. Since, in linear perturbation theory (reference 2),

$$\frac{\partial \varphi}{\partial x} = V_0 \frac{\partial u}{\partial x}, \quad \frac{\partial \varphi}{\partial y} = V_0 \frac{\partial v}{\partial x}, \quad \frac{\partial \varphi}{\partial z} = V_0 \frac{\partial w}{\partial x} \quad (20)$$

where  $u$ ,  $v$ ,  $w$  are respectively the  $x$ ,  $y$ ,  $z$  components of the perturbation velocities, it follows that

$$\begin{aligned} u &= \frac{1}{V_0} \varphi \\ v &= \frac{\partial}{\partial y} \int_{-\infty}^x \frac{1}{V_0} \varphi(x_1, y, z) dx_1 \\ w &= \frac{\partial}{\partial z} \int_{-\infty}^x \frac{1}{V_0} \varphi(x_1, y, z) dx_1 \end{aligned} \quad (21)$$

The induced velocities for the infinite span airfoil result immediately from equations (19) and (21). If the upper sign of a double sign is again referred to the  $z > 0$  case, the results may be written in the form

$$\left. \begin{aligned} u &= \pm \frac{C_0}{2V_0} \\ v &= 0 \\ w &= -\frac{C_0}{2V_0} \sqrt{M_0^2 - 1} \end{aligned} \right\} \text{ for } 0 \leq x \mp \beta z \leq c \quad (22)$$

Since the vertical induced velocities are constant, it follows that the supersonic airfoil of infinite aspect ratio and uniform load distribution is a flat plate. The relations between this loading and angle of attack will be considered later.

**Lifting surface with rectangular plan form.** The complete discussion of the supersonic lifting surface with uniform loading and rectangular plan form is lengthened considerably by the fact that in calculating the acceleration potential at the point  $P$  with coordinates  $x$ ,  $y$ ,  $z$  it is necessary to distinguish between several regions in space in which the point may be located. These regions arise from consideration of the manner in which the forecone of the point  $P$  cuts the surface of discontinuity. The value of  $\varphi$  can be found with approximately equal facility in each of these regions but, since this paper is concerned primarily with effects on the surface of the airfoil, the solutions for pertinent regions only will be given here.

Figure 4 shows the rectangular plan form  $LL'T'T'$  together with the coordinate system to be used. The dimensions of the wing are chosen so that the Mach cones extending back from the leading edge will not intersect within the boundaries of the wing. This restriction, which is not necessary but merely simplifies the analysis, implies that if  $b$  is the span of the wing and  $c$  the chord length, then

$$\tan \mu = \frac{1}{\sqrt{M_0^2 - 1}} < \frac{b}{2c} \quad (23)$$

where  $\mu = \arcsin \frac{1}{M_0}$  is the so-called Mach angle of the stream and equal to the semivertex angles of the Mach cones.

The loading over the rectangular plan form is to be uniform so the expression  $\varphi_u - \varphi_t$  is set equal to  $C_0$  for  $-\frac{1}{2}b \leq y_1 \leq \frac{1}{2}b$  and  $0 \leq x_1 \leq c$ . The acceleration potential, expressed as a function of  $x$ ,  $y$ ,  $z$ , is thus obtainable from equation (17) and the limits of integration must be determined from the position of  $P$ . From reasons of symmetry, only the portion of space for which  $y \geq 0$  need be considered. Once the acceleration potential has been calculated, equations (21) may be used to calculate induced velocities. The results of such calculations are given and the same convention for double signs is used.

**Region I:** Behind the leading-edge wedge, ahead of the trailing-edge wedge, and bounded laterally by the  $y=0$

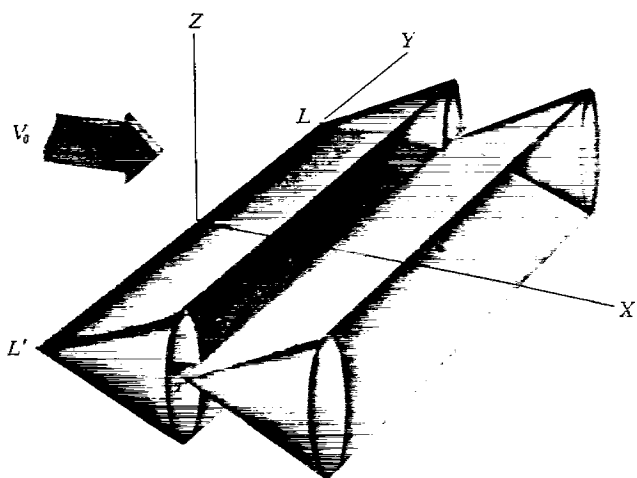


FIGURE 4.—Lifting surface with Mach cones and coordinate system for rectangular plan form.

plane and the Mach cone from the leading-edge tip. The results in this region correspond to results obtained for the infinite span airfoil. Thus

$$\begin{aligned}\varphi &= \pm \frac{1}{2} C_0 \\ u &= \pm C_0 / 2V_0 \\ v &= 0 \\ w &= -\frac{C_0}{2V_0} \beta\end{aligned}\quad (24)$$

Region  $I_2$ : Within the Mach cone from the leading-edge tip, outside the Mach cone from the trailing-edge tip, and forward of the trailing-edge wedge. Denoting the integrand in equation (17) by the symbol  $I$ , the expression for  $\varphi$ , when

$y < \frac{1}{2} b$ , is

$$\varphi(x, y, z) = +\frac{1}{2\pi} \frac{\partial}{\partial x} \left( \int_0^{X_1} dx_1 \int_{Y_1}^{\frac{1}{2}b} I dy_1 + \int_{X_1}^{X_2} dx_1 \int_{Y_1}^{Y_2} I dy_1 \right) \quad (25)$$

where

$$Y_1 = y - \frac{1}{\beta} \sqrt{(x-x_1)^2 - \beta^2 z^2}, \quad X_1 = x - \beta \sqrt{\left(y - \frac{1}{2} b\right)^2 + z^2}$$

$$Y_2 = y + \frac{1}{\beta} \sqrt{(x-x_1)^2 - \beta^2 z^2}, \quad X_2 = x \mp \beta z$$

Application of equations (21), after integrating either equation (25) or its companion expression when  $y > \frac{1}{2} b$ , yields the results:

$$\varphi = \frac{C_0}{2\pi} \left\{ \pm \frac{\pi}{2} - \arctan \frac{x \left(y - \frac{1}{2} b\right)}{z \sqrt{x^2 - \beta^2 \left[\left(y - \frac{1}{2} b\right)^2 + z^2\right]}} \right\}$$

$$\begin{aligned}u &= \frac{C_0}{2\pi V_0} \left\{ \pm \frac{\pi}{2} - \arctan \frac{x \left(y - \frac{1}{2} b\right)}{z \sqrt{x^2 - \beta^2 \left[\left(y - \frac{1}{2} b\right)^2 + z^2\right]}} \right\} \\ v &= \frac{C_0}{2\pi V_0} \frac{-z}{\left(y - \frac{1}{2} b\right)^2 + z^2} \sqrt{x^2 - \beta^2 \left[\left(y - \frac{1}{2} b\right)^2 + z^2\right]} \\ w &= \frac{C_0}{2\pi V_0} \left\{ -\frac{\beta\pi}{2} + \beta \arctan \frac{\beta \left(y - \frac{1}{2} b\right)}{\sqrt{x^2 - \beta^2 \left[\left(y - \frac{1}{2} b\right)^2 + z^2\right]}} + \right. \\ &\quad \left. \frac{\left(y - \frac{1}{2} b\right)}{\left(y - \frac{1}{2} b\right)^2 + z^2} \sqrt{x^2 - \beta^2 \left[\left(y - \frac{1}{2} b\right)^2 + z^2\right]} \right\}\end{aligned}\quad (26)$$

As a partial check of the expression for  $\varphi$  in equations (26), it can be seen that in the limit as  $z$  approaches zero the value of  $\varphi$  agrees with the result given in equation (24) on the wing while the value is zero off the wing.

The values of vertical induced velocity in the plane  $z=0$  are of particular interest since from a knowledge of the distribution of  $w$  the surface shape and local angle of attack corresponding to the imposed load distribution can be determined. The expressions for  $w$  for uniform loading will be particularly useful later when the load distribution is modified in order to obtain airfoils with specified induced velocities. Introducing the notation

$$\eta = \frac{\left(y - \frac{1}{2} b\right) \beta}{x} \quad (27)$$

the following results are obtained for the area covered by the tip cone:

For  $0 < \eta < 1$ ,

$$w_{z=0} = \frac{-C_0 \beta}{2\pi V_0} \int_1^\eta \frac{\sqrt{1-\eta_1^2}}{\eta_1^2} d\eta_1 \quad (28)$$

and for  $-1 < \eta < 0$ , ( $x < c$ )

$$w_{z=0} = \frac{-C_0 \beta}{2\pi V_0} \left( \pi + \int_{-1}^\eta \frac{\sqrt{1-\eta_1^2}}{\eta_1^2} d\eta_1 \right)$$

After integration of these two expressions, the explicit value of vertical induced velocity throughout the entire region is found to be

$$w_{z=0} = \frac{C_0 \beta}{2\pi V_0} \left( -\frac{\pi}{2} + \frac{\sqrt{1-\eta^2}}{\eta} + \arcsin \eta \right) \quad (29)$$

Equations (28) and (29) indicate that the flow over the tip portion of the airfoil is of the type referred to as "conical flow." For this type of flow the values of induced downwash, aerodynamic loading, etc., are functions merely of the angle  $\eta$ .

Busemann (reference 7), Stewart (reference 8), and Lagerstrom (reference 9) have developed analyses for certain plan forms which are postulated on the existence of this type of solution. In all cases for which the flow field is conical the problem is effectively two-dimensional. Such a simplification reduces the analysis in this report to a consideration of a single integral equation while in the references just mentioned complex variable theory can be applied directly.

**Tip of swept-forward lifting surface.**—Consider the tip of a swept-forward supersonic lifting surface with uniform loading (fig. 5), the angle  $\delta_0$  between the leading edge and the  $x$  axis and the angle  $\delta_1$  between the trailing edge and the  $x$  axis both being less than the free-stream Mach angle  $\mu$ .

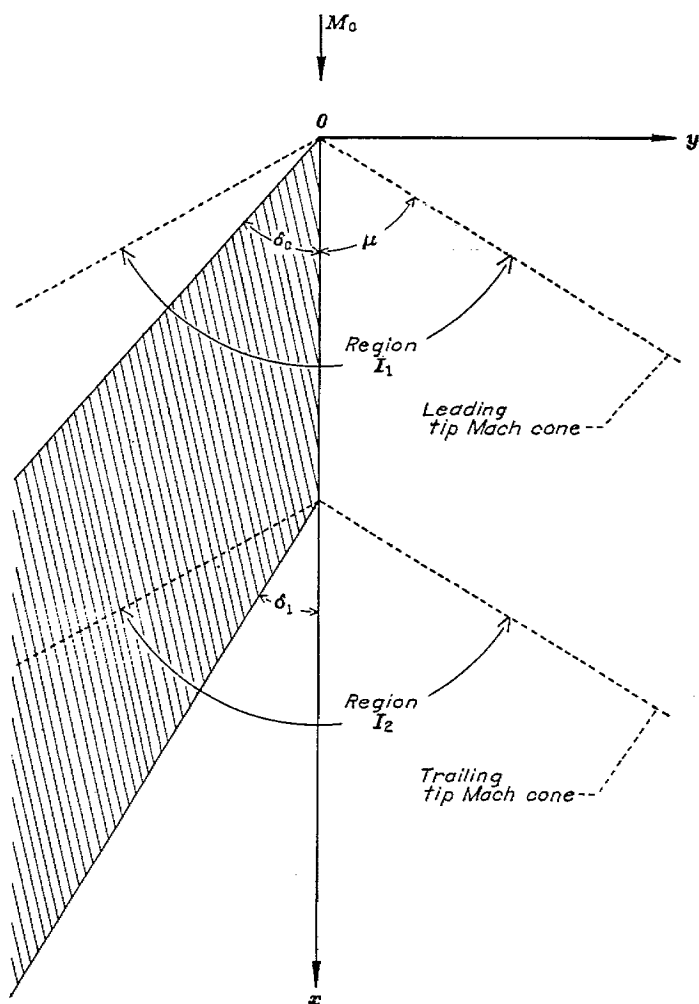


FIGURE 5.—Tip of swept-forward lifting surface with traces of Mach cones, coordinate system, and regions defined for equations (32) and (34).

In carrying out the integrations it is necessary to distinguish between the type in which the tip boundaries are behind the Mach cones and the type in which the tip boundaries are ahead. The analyses of these two cases are of equivalent complexity, however, and can be handled with equal facility by the methods outlined. For all surfaces whose leading edges form an apex, only the case where the wing boundaries are behind the Mach cone will be considered. A Cartesian coordinate system is chosen as shown so that the origin

lies at the apex, the positive  $x$  axis extending downstream, the  $y$  axis extending laterally, and the  $z$  axis being directed normal to the plane of the plan form and to the free-stream direction. The equations of the sides of the lifting surface are

$$y=0$$

$$y=-x \tan \delta_0 = -\frac{\theta_0}{\beta} x$$

and

$$y=-(x-c) \tan \delta_1 = -\frac{\theta_1}{\beta} (x-c)$$

The calculation of  $\varphi(x, y, z)$  again must be divided into cases depending upon the location of the point  $P: (x, y, z)$ . In the results listed below are included the explicit expressions for  $\varphi(x, y, z)$ ; the induced velocities, however, are given only in the plane  $z=0$ , as the integration to obtain a general expression is difficult. The velocities in the  $z=0$  plane, which are sufficient for the purpose of this investigation, can be obtained from a simpler integration since, for the integral involved,

$$\lim_{z \rightarrow 0} \int I(x, y, z) dx = \int I(x, y, 0) dx$$

This simplification was used in the analysis of most of the lifting surfaces investigated. As before, it is assumed that the discontinuity in  $\varphi$  is equal to  $C_0$ . Moreover, the expressions for  $w_{z=0}$  are given in terms of the variables  $\eta$  and  $\omega$  where

$$\eta = \frac{\beta y}{x} \text{ and } \omega = 1 - \frac{c}{x} \quad (30)$$

In this manner the solution is shown to be conical in the region ahead of the trailing-tip Mach cone (fig. 5). For points behind this Mach cone the flow is not conical but a function of both  $\eta$  and  $\omega$ .

**Region  $I_1$ :** Inside the leading-tip Mach cone and ahead of the trailing-tip Mach cone. Integration of equation (17) yields the result

$$\varphi = \frac{C_0}{2\pi} \left[ -\arctan \frac{xy}{z\sqrt{x^2 - \beta^2(y^2 + z^2)}} + \arctan \frac{xy + x^2 \frac{\theta_0}{\beta} - \beta z^2 \theta_0}{z\sqrt{x^2 - \beta^2(y^2 + z^2)}} \right] \quad (31)$$

and, after further calculation,

$$\begin{aligned} w_{z=0} &= -\frac{C_0 \beta \theta_0}{2\pi V_0} \int_{-1}^{\eta} \frac{\sqrt{1-\eta_1^2}}{\eta_1^2 (\eta_1 + \theta_0)} d\eta_1, \quad -1 < \eta < 0 \\ &= -\frac{C_0 \beta \theta_0}{2\pi V_0} \int_1^{\eta} \frac{\sqrt{1-\eta_1^2}}{\eta_1^2 (\eta_1 + \theta_0)} d\eta_1, \quad 0 < \eta < 1 \\ &= \frac{C_0 \beta}{2\pi V_0} \left[ \frac{\sqrt{1-\eta^2}}{\eta} - \frac{1}{\theta_0} \operatorname{arcosh} \frac{1}{|\eta|} + \right. \\ &\quad \left. \frac{\sqrt{1-\theta_0^2}}{\theta_0} \operatorname{arcosh} \frac{(1+\theta_0\eta)}{|\theta_0+\eta|} \right], \quad -1 < \eta < 1 \quad (32) \end{aligned}$$



Region  $I_2$ : Inside both tip Mach cones. The solution in this region is simplified through use of the fact that for linear differential equations any algebraic sum of solutions will be another solution of the equation. Since the differential equation for the acceleration potential is linear, this property can be applied to obtain a solution for the region  $I_2$  by subtracting from the expressions given for region  $I_1$  corresponding expressions in which the variable  $\delta_1$  replaces  $\delta_0$  and  $(x-c)$  replaces  $x$ . Thus

$$\varphi = \frac{C_0}{2\pi} \left[ -\arctan \frac{xy}{z\sqrt{x^2 - \beta^2(y^2 + z^2)}} + \arctan \frac{xy + x^2 \frac{\theta_0}{\beta} - \beta z^2 \theta_0}{z\sqrt{x^2 - \beta^2(y^2 + z^2)}} + \right. \\ \left. \arctan \frac{(x-c)y}{z\sqrt{(x-c)^2 - \beta^2(y^2 + z^2)}} - \arctan \frac{(x-c)y + (x-c)^2 \frac{\theta_1}{\beta} - \beta z^2 \theta_1}{z\sqrt{(x-c)^2 - \beta^2(y^2 + z^2)}} \right] \quad (33)$$

and for  $-1 < \eta < 1$

$$w_{z=0} = \frac{C_0 \beta}{2\pi V_0} \left[ \frac{\sqrt{1-\eta^2}}{\eta} - \frac{1}{\theta_0} \operatorname{arccosh} \frac{1}{|\eta|} + \right. \\ \left. \frac{\sqrt{1-\theta_0^2}}{\theta_0} \operatorname{arccosh} \frac{(1+\theta_0\eta)}{[(\theta_0+\eta)]} - \frac{\sqrt{\omega^2-\eta^2}}{\eta} + \frac{1}{\theta_1} \operatorname{arccosh} \frac{|\omega|}{|\eta|} - \right. \\ \left. \frac{\sqrt{1-\theta_1^2}}{\theta_1} \operatorname{arccosh} \frac{|\omega+\theta_1\eta|}{|\theta_1\omega+\eta|} \right] \quad (34)$$

**Lifting surface with trapezoidal plan form.**—The linear property of the differential equation may be used to advantage in determining the flow about a trapezoidal lifting surface with uniform lift distribution, since the boundary conditions within the plan form of the airfoil are obviously satisfied when the acceleration potential for a triangular tip is subtracted from the potential for the rectangular surface.

Suppose (fig. 6) the angle of rake of the trapezoid is  $\delta_0$  and that  $\delta_0$  is less than the Mach angle  $\mu$ . The acceleration potential will be identical, over the central portion of the surface, to that for the lifting surface of infinite aspect ratio. Over the parts of the surface which are blanketed by the tip Mach cones the flow will, however, be modified. Because of symmetry the determination of this modification need only be carried out on one side of the figure.

If the coordinate axes are chosen as shown in figure 6, the lateral boundary of the lifting surface is

$$y = -x \tan \delta_0 = -\frac{\theta_0 x}{\beta}$$

It has been shown that both the rectangular plan form and the triangular plan form experience conical-type flow over the region within the tip Mach cones. Thus, the variable  $\eta$  defined in equation (30) may be used.

Region  $I_1$ : Inside the Mach cone originating at the leading-edge tip, outside the Mach cone from the trailing-edge tip, forward of the trailing-edge wedge, and to the left of the  $y=0$  plane.

For  $-1 < \eta < 0$ :

$$w_{z=0} = \frac{C_0 \beta}{2\pi V_0} \left( -\pi - \int_{-1}^{\eta} \frac{\sqrt{1-\eta_1^2}}{\eta_1} \frac{d\eta_1}{\eta_1 + \theta_0} \right) \\ = \frac{C_0 \beta}{2\pi V_0} \left[ -\frac{\pi}{2} + \arctan \frac{\eta}{\sqrt{1-\eta^2}} + \frac{1}{\theta_0} \operatorname{arccosh} \frac{1}{|\eta|} - \right. \\ \left. \frac{\sqrt{1-\theta_0^2}}{\theta_0} \operatorname{arccosh} \frac{(1+\theta_0\eta)}{[(\theta_0+\eta)]} \right] \quad (35)$$

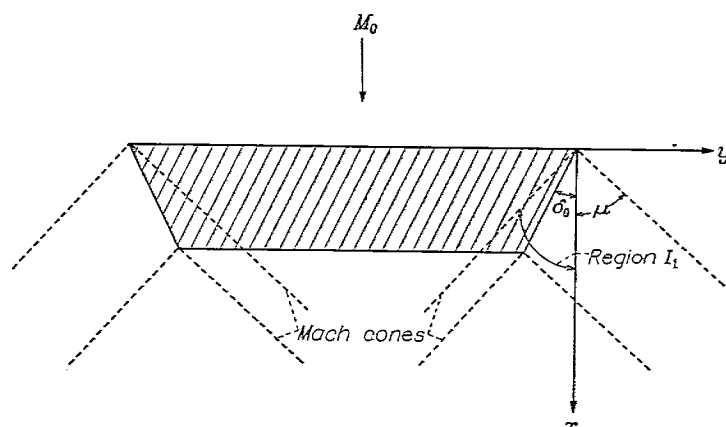


FIGURE 6.—Trapezoidal lifting surface with traces of Mach cones, coordinate system, and regions defined for equation (35).

**Swept-back lifting surface.**—As another example of the way in which the linearity of the differential equation may be utilized to obtain further solutions, the induced vertical velocities for a swept-back wing will be determined for the case in which the leading and trailing edges lie behind their respective Mach cones (fig. 7). The boundaries of the plan form are given by the equations

$$y = -\frac{\theta_0}{\beta} x, \quad y = \frac{\theta_0}{\beta} x \\ y = -\frac{\theta_1}{\beta} (x-c), \quad y = \frac{\theta_1}{\beta} (x-c)$$

The flow will be conical ahead of the trailing-edge Mach cone where the induced velocities can be expressed in terms of the variable  $\eta$ . Behind the trailing-edge Mach cone the flow will not be conical but will be expressible in terms of the variables  $\eta$  and  $\omega = 1 - \frac{c}{x}$ .

Consider first the region of conical flow. In order to determine  $w_{z=0}$  for a given value of  $\eta$  it is possible to consider separately the induced effects produced by each half of the surface. But in the region ahead of the trailing-edge Mach cone, the induced velocities arising from one half of the surface are given by the formula for a similar region on the swept-forward surface. For reasons of symmetry the results for the entire swept-back lifting surface need only be given for values of  $\eta$  within the limits  $-1 < \eta < 0$ .

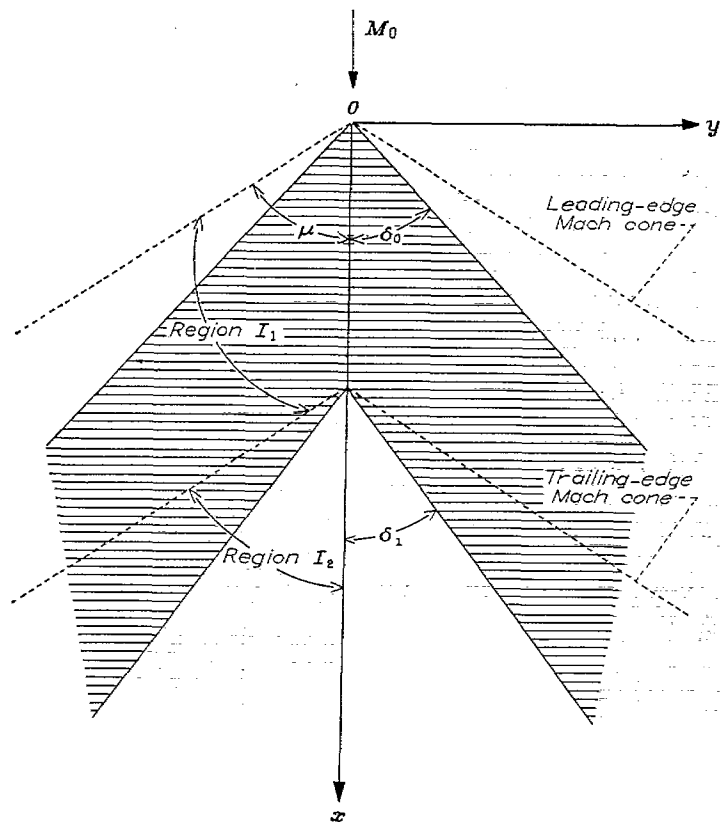


FIGURE 7.—Swept-back lifting surface with traces of Mach cones, coordinate system, and regions defined for equations (36) and (37).

In the region where the flow is not conical the solution will be built up of a combination of solutions obtained from the regions of conical flow.

Region  $I_1$ : Inside the leading-edge Mach cone, outside the trailing-edge Mach cone, and to the left of the  $y=0$  plane. For  $-1 < \eta < 0$

$$w_{z=0} = \frac{\beta C_0 \theta_0}{2\pi V_0} \int_{-1}^{\eta} \frac{\sqrt{1-\eta_1^2}}{\eta_1} \frac{2}{\theta_0^2 - \eta_1^2} d\eta_1 \quad (36)$$

$$= \frac{C_0 \beta}{2\pi V_0} \left[ -\frac{2}{\theta_0} \operatorname{arc} \cosh \frac{1}{|\eta|} + \frac{\sqrt{1-\theta_0^2}}{\theta_0} \operatorname{arc} \cosh \frac{(2-\theta_0^2-\eta^2)}{[(\theta_0^2-\eta^2)]} \right]$$

Region  $I_2$ : Inside both Mach cones and to the left of the  $y=0$  plane. The solution in this region can be produced by subtracting from the value of  $w_{z=0}$  given for region  $I_1$  the value of  $w_{z=0}$  given for the same region except that in the latter case  $\delta_0$  is replaced by  $\delta_1$  and  $x$  by  $(x-c)$ . Thus,

$$w_{z=0} = \frac{C_0 \beta}{2\pi V_0} \left[ -\frac{2}{\theta_0} \operatorname{arc} \cosh \left| \frac{1}{\eta} \right| + \frac{\sqrt{1-\theta_0^2}}{\theta_0} \operatorname{arc} \cosh \frac{(2-\theta_0^2-\eta^2)}{[(\theta_0^2-\eta^2)]} + \frac{2}{\theta_1} \operatorname{arc} \cosh \left| \frac{\omega}{\eta} \right| - \frac{\sqrt{1-\theta_1^2}}{\theta_1} \operatorname{arc} \cosh \left| \frac{(2-\theta_1^2)\omega^2-\eta^2}{(\eta^2-\theta_1^2\omega^2)} \right| \right] \quad (37)$$

Although the uniformly loaded lifting surface was the only prescribed loading analyzed, it should be noted that the basic integration leading to a solution of this type of problem (equation (17)) is in no way restricted to a uniform load. Arbitrary loadings that may or may not be analytic functions of  $x$  and  $y$  can be specified and the problem therefore becomes

one of technique in integration. The solutions for the uniformly loaded surfaces, however, are particularly useful. By methods of superposition these solutions can be used to obtain the surface loading for specified plan forms (the inverse problem) as will be illustrated in the following section.

#### LOAD DISTRIBUTIONS ON FLAT-PLATE LIFTING SURFACES IN SUPERSONIC FLOW

**Infinite span wing.**—Since the vertical induced velocity is constant for the supersonic airfoil of infinite aspect ratio (equation (22)) and uniform load, it follows that the airfoil is a flat plate. This property distinguishes the infinite aspect ratio problem from all other plan forms considered, for the load distribution must be modified in the latter cases so that twist and camber are removed from the wing to obtain a flat plate.

Denoting the angle of attack of the airfoil by  $\alpha$ ,

$$\alpha = -\frac{w_{z=0}}{V_0} = \frac{C_0}{2V_0^2} \sqrt{M_0^2-1} \quad (38)$$

Moreover,

$$p_l - p_u = \rho_0 (\varphi_u - \varphi_l) = \rho_0 C_0$$

and, setting

$$\frac{p_l - p_u}{\frac{1}{2} \rho_0 V_0^2} = \frac{\Delta p}{q}$$

it follows that

$$\frac{\Delta p}{q} = \frac{2C_0}{V_0^2} \quad (39)$$

Eliminating  $C_0$  between equations (38) and (39),

$$\frac{\Delta p}{q} = \frac{4\alpha}{\sqrt{M_0^2-1}} \quad (40)$$

The result given in equation (40) is the well-known Ackeret expression developed in reference 10. The derivation here follows the approach of Prandtl (reference 2).

**Rectangular plan form.**—Since the vertical induced velocity for the uniformly loaded supersonic airfoil of rectangular plan form is not constant over the portion of the wing covered by the tip Mach cones, it is necessary to modify the load distribution within this region in order to get a flat plate. The determination of the required load distribution will be shown to depend on the solution of an integral equation and subsequent problems dealing with other plan forms will, from a mathematical standpoint, be similar in form.

The rectangular plan form will be thought of as being built of superimposed trapezoidal lifting surfaces with variable angles of rake (fig. 8), each trapezoidal surface having a uniform load distribution but with loading allowed to vary with the variable rake angle  $\delta$ .

Since the flow over the part of the airfoil within the Mach cone is conical, it is possible to express  $w_{z=0}$  as a function of  $\eta$  where

$$\eta = \frac{\beta y}{x}$$

Setting

$$\beta \tan \delta = \theta$$

and using equation (35)

$$\frac{2\pi V_0 w(\eta)_{z=0}}{\beta} = \int_{\theta=0}^{\theta=1} C'(\theta) \left( -\pi - \int_{-1}^{\eta} \frac{\sqrt{1-\eta_1^2}}{\eta_1} \frac{d\eta_1}{\eta_1+\theta} \right) d\theta \quad (41)$$

where  $C'(\theta) = \varphi_u - \varphi_l$  for the single trapezoidal surface with rake angle  $\delta$ .

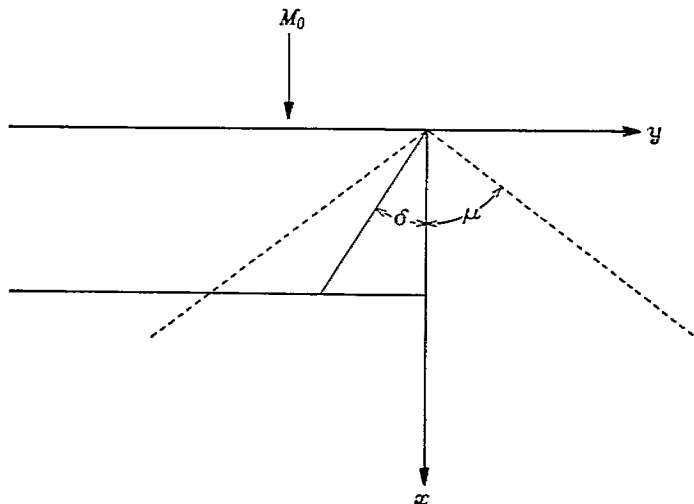


FIGURE 8.—Rectangular plan form built of superimposed trapezoidal lifting surfaces with variable rake.

The solution of the problem depends on the determination of a function  $C'(\theta)$  which, when substituted in equation (41), will yield a constant value of  $w_{z=0}(\eta)$ ; that is, a value of  $w_{z=0}$  independent of the variable  $\eta$ . Imposing the condition that

$$\frac{dw_{z=0}}{d\eta} = 0$$

the problem is resolved into one of solving the equation

$$0 = \frac{d}{d\eta} \int_{\theta=0}^{\theta=1} C'(\theta) d\theta \int_{-1}^{\eta} \frac{\sqrt{1-\eta_1^2}}{\eta_1} \frac{d\eta_1}{\eta_1+\theta}$$

By means of the notation

$$\int_{-1}^{\eta} \frac{\sqrt{1-\eta_1^2}}{\eta_1} \frac{d\eta_1}{\eta_1+\theta} = G_1(\eta, \theta)$$

the integral equation is written in the form

$$0 = \lim_{\epsilon \rightarrow 0} \left[ \frac{d}{d\eta} \int_{\theta=0}^{\theta=1-\epsilon} C'(\theta) G_1(\eta, \theta) d\theta + \frac{d}{d\eta} \int_{\theta=-\eta+\epsilon}^{\theta=1} C'(\theta) G_1(\eta, \theta) d\theta \right]$$

where the singularity in the integrand necessitates the use of the infinitesimal  $\epsilon$ . The evaluation of the derivative thus leads to the expression

$$0 = \lim_{\epsilon \rightarrow 0} \left[ \int_0^{-\eta-\epsilon} C'(\theta) \frac{\partial G_1}{\partial \eta} d\theta + \int_{-\eta+\epsilon}^1 C'(\theta) \frac{\partial G_1}{\partial \eta} d\theta - C'(-\eta-\epsilon) G_1(\eta, -\eta-\epsilon) + C'(-\eta+\epsilon) G_1(\eta, -\eta+\epsilon) \right]$$

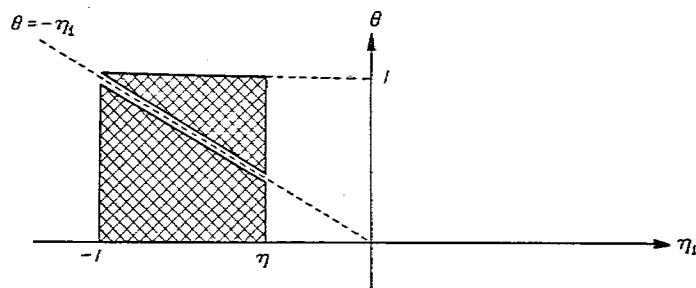


FIGURE 9.—Region of integration showing line of singularity for equation (44).

It can be shown from equation (35) that, if  $C'(\theta)$  is a continuous function,

$$\lim_{\epsilon \rightarrow 0} \left[ -C'(-\eta-\epsilon) G_1(\eta, -\eta-\epsilon) + C'(-\eta+\epsilon) G_1(\eta, -\eta+\epsilon) \right] = 0$$

Hence

$$0 = \frac{\sqrt{1-\eta_1^2}}{\eta_1} \int_0^1 \frac{C'(\theta) d\theta}{\eta_1+\theta} \quad (42)$$

and the solution of this equation is

$$C'(\theta) = \frac{C_1}{\sqrt{\theta(1-\theta)}} \quad (43)$$

where  $C_1$  is a constant to be determined later. Substituting from equation (43) into equation (41)

$$\frac{2\pi V_0 w(\eta)_{z=0}}{\beta C_1} = - \int_0^1 \frac{\pi d\theta}{\sqrt{\theta(1-\theta)}} - \int_0^1 \frac{d\theta}{\sqrt{\theta(1-\theta)}} \int_{-1}^{\eta} \frac{\sqrt{1-\eta_1^2}}{\eta_1(\eta_1+\theta)} d\eta_1 \quad (44)$$

The region of integration in the  $\eta_1\theta$  plane for the double integral of equation (44) is shown as the cross-hatched area of figure 9, a singularity in the integrand occurring along the line  $\theta = -\eta_1$ . Rewriting the equation and reversing the order of integration in the double integral,

$$\frac{2\pi V_0 w(\eta)_{z=0}}{\beta C_1} = -2\pi \arcsin \sqrt{\theta} \Big|_0^1 - \lim_{\epsilon \rightarrow 0} \int_{-1}^{\eta} \frac{\sqrt{1-\eta_1^2}}{\eta_1} d\eta_1 \left[ \int_0^{-\eta-\epsilon} \frac{d\theta}{(\eta_1+\theta)\sqrt{\theta(1-\theta)}} + \int_{-\eta+\epsilon}^1 \frac{d\theta}{(\eta_1+\theta)\sqrt{\theta(1-\theta)}} \right]$$

The bracketed expression in this equation can be shown to vanish for all values of  $\eta_1$  between zero and  $-1$  so that, finally,

$$w_{z=0} = \frac{-C_1\beta}{2\pi V_0} 2\pi \arcsin \sqrt{\theta} \Big|_0^1 = \frac{-C_1\beta\pi}{2V_0} \quad (45)$$

Since the trapezoidal lifting surfaces are superimposed, the loading  $C(\theta)$  over the resultant rectangular plan form satisfies the relation

$$\frac{dC(\theta)}{d\theta} = C'(\theta) = \frac{C_1}{\sqrt{\theta(1-\theta)}}$$

Imposing the condition that  $C(\theta)=0$  at  $\theta=0$ , it follows that

$$C(\theta)=2C_1 \arcsin \sqrt{\theta} \quad (46)$$

This equation gives the incremental change of acceleration potential between the upper and lower lifting surface of the rectangular wing. As a result the increment in pressure is

$$p_t - p_u = \rho_0(\varphi_u - \varphi_t) = 2\rho_0 C_1 \arcsin \sqrt{\theta}$$

Expressing the pressure difference in nondimensional terms,

$$\frac{p_t - p_u}{\frac{1}{2} \rho_0 V_0^2} = \frac{\Delta p}{q} = \frac{4C_1}{V_0^2} \arcsin \sqrt{\theta} \quad (47)$$

The constant  $C_1$  may be eliminated between equations (45) and (47) and as a consequence

$$\frac{\Delta p}{q} = -\frac{w_{z=0}}{V_0} \frac{8}{\beta \pi} \arcsin \sqrt{\theta}$$

Since the angle of attack  $\alpha$  of the airfoil is by definition equal to  $-\frac{w_{z=0}}{V_0}$ , the final expression for the loading, in coefficient form, over the outer portions of the rectangular wing is

$$\frac{\Delta p}{q} = \frac{8\alpha}{\pi \sqrt{M_0^2 - 1}} \arcsin \sqrt{\theta} \quad (48)$$

The general approach used to obtain this result is similar to that used by Schlichting (reference 11). The error in Schlichting's final result has been noted by Busemann and others.

Lift coefficient  $C_L$  for an arbitrary wing is defined by the relation

$$C_L = \frac{L}{S_0 q} = \frac{1}{S_0} \int \int \frac{\Delta p}{q} dS \quad (49)$$

where

$L$ =total lift of the wing

$dS$ =element of area on the wing

$S_0$ =total area of wing

For the rectangular wing the values of  $\Delta p/q$  over the tip and center sections are given by equations (48) and (40). As a result of this integration

$$C_L = \frac{4\alpha}{\beta} \left(1 - \frac{1}{2\beta A}\right) \quad (50)$$

where  $A$  is the aspect ratio and by definition equal to the ratio of the square of the span and the wing area. As a final conclusion the lift-curve slope of the wing is

$$\frac{dC_L}{d\alpha} = \frac{4}{\beta} \left(1 - \frac{1}{2\beta A}\right) \quad (51)$$

**Trapezoidal plan form.**—The results given in equations (48) and (51) are capable of generalization to the case of the flat plate having trapezoidal plan form and with rake angle  $\delta_0$  less than the Mach angle of the stream. For such a configuration the airfoil is again blanketed in part by the tip Mach cones and the loading in this outer section of the

airfoil must be adjusted properly to give constant induced vertical velocity. Superposition of trapezoidal lifting surfaces with loadings varying with rake angle  $\delta$  can again be used and the conical nature of the flow employed. Setting

$$\eta = \beta y/x$$

$$\theta = \beta \tan \delta$$

$$\theta_0 = \beta \tan \delta_0$$

equation (35) leads to the expression

$$\frac{2\pi V_0 w(\eta)_{z=0}}{\beta} = \int_{\theta=\theta_0}^{\theta=1} C'(\theta) \left( -\pi - \int_{-1}^{\eta} \frac{\sqrt{1-\eta_1^2}}{\eta_1} \frac{d\eta_1}{\eta_1 + \theta} \right) d\theta \quad (52)$$

where  $C'(\theta) = \varphi_u - \varphi_t$  for the single trapezoidal surface with rake angle  $\delta$ .

The analysis in this case follows along lines directly analogous to that used for the rectangular surface. For the present configuration the loading function for the superimposed trapezoids is given by the relation

$$C'(\theta) = \frac{C_1}{\sqrt{(\theta - \theta_0)(1 - \theta)}} \quad (53)$$

and the integration to obtain  $w_{z=0}$  can be simplified to give, as a final result,

$$w_{z=0} = -\frac{\beta C_1}{2\pi V_0} \int_{\theta_0}^1 \frac{\pi d\theta}{\sqrt{(\theta - \theta_0)(1 - \theta)}} = -\frac{C_1 \beta \pi}{2V_0} \quad (54)$$

The loading  $C(\theta)$  over the resultant trapezoidal plan form can be found from the relation

$$\frac{dC(\theta)}{d\theta} = \frac{C_1}{\sqrt{(\theta - \theta_0)(1 - \theta)}}$$

From the boundary condition that  $C(\theta)=0$  at  $\theta=\theta_0$  it follows that

$$C(\theta) = 2C_1 \arcsin \sqrt{\frac{\theta - \theta_0}{1 - \theta_0}}$$

and

$$\frac{p_t - p_u}{\frac{1}{2} \rho_0 V_0^2} = \frac{\Delta p}{q} = \frac{4C_1}{V_0^2} \arcsin \sqrt{\frac{\theta - \theta_0}{1 - \theta_0}} \quad (55)$$

Elimination of  $C_1$  between equations (54) and (55) and introduction of angle of attack  $\alpha$  for  $-w_{z=0}/V_0$  gives as aerodynamic loading over the portion of the airfoil within the tip Mach cones the expression

$$\frac{\Delta p}{q} = \frac{8\alpha}{\pi \beta} \arcsin \sqrt{\frac{\theta - \theta_0}{1 - \theta_0}}, \quad 0 \leq \theta \leq 1 \quad (56)$$

Figure 10 indicates the variation of the loading over the tip section of the trapezoid. The variable  $(\beta/\alpha)(\Delta p/q)$  is plotted against  $\beta \tan \delta$  for  $\beta \tan \delta_0$  equal to 0, 0.3, and 0.6. The curve for  $\beta \tan \delta_0=0$  corresponds to the case of the rectangular wing and shows results in agreement with equation (48).



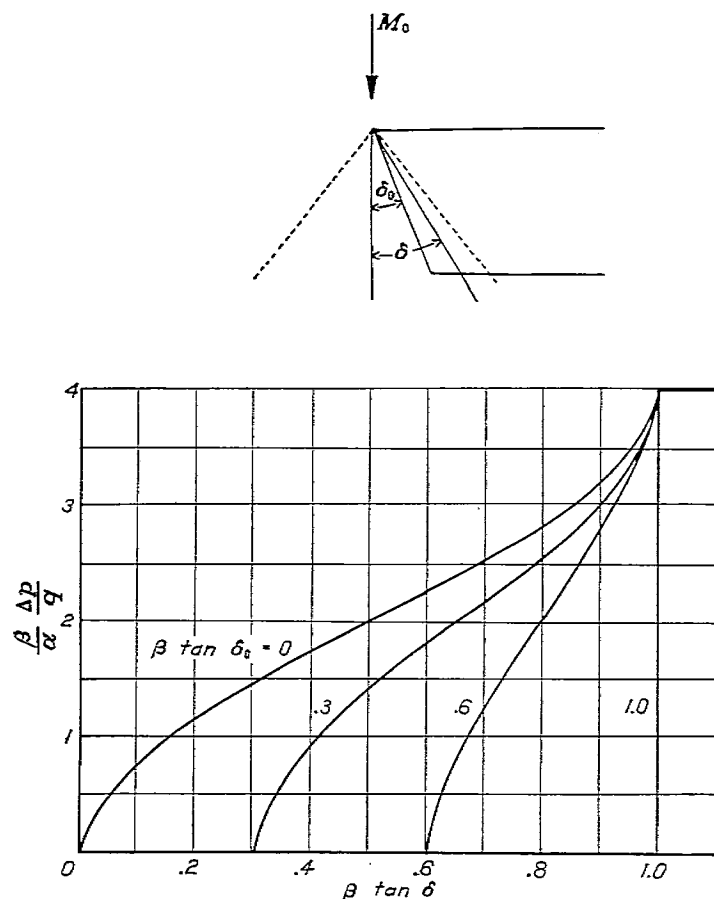


FIGURE 10.—Load distribution over tip for various trapezoidal plan forms.

By means of equation (49) together with equations (56) and (40) the lift coefficient of the trapezoidal wing is expressible in the form

$$C_L = \frac{4\alpha}{\beta} \left( \frac{1 - \frac{c}{2b} \tan \delta_0 - \frac{c}{2b} \tan \mu}{1 - \frac{c}{b} \tan \delta_0} \right) \quad (57)$$

Introducing the aspect ratio  $A$  of the wing where

$$A = \frac{b}{c \left( 1 - \frac{c}{b} \tan \delta_0 \right)}$$

one gets for lift coefficient the relation

$$C_L = \frac{2\alpha}{\beta} \left[ 1 + \frac{Ac}{b} \left( 1 - \frac{c}{\beta b} \right) \right] \quad (58)$$

From equation (57),

$$\frac{dC_L}{d\alpha} = \frac{4}{\beta} \left( \frac{1 - \frac{c}{2b} \tan \delta_0 - \frac{c}{2b} \tan \mu}{1 - \frac{c}{b} \tan \delta_0} \right) \quad (59)$$

In figure 11,  $\beta \frac{dC_L}{d\alpha}$  is plotted as a function of  $A\beta$  for  $\theta_0 = 0, \frac{1}{2},$

and 1. The curve for  $\theta_0 = 0$  agrees with results given by equation (51) for the rectangular wing. All curves are

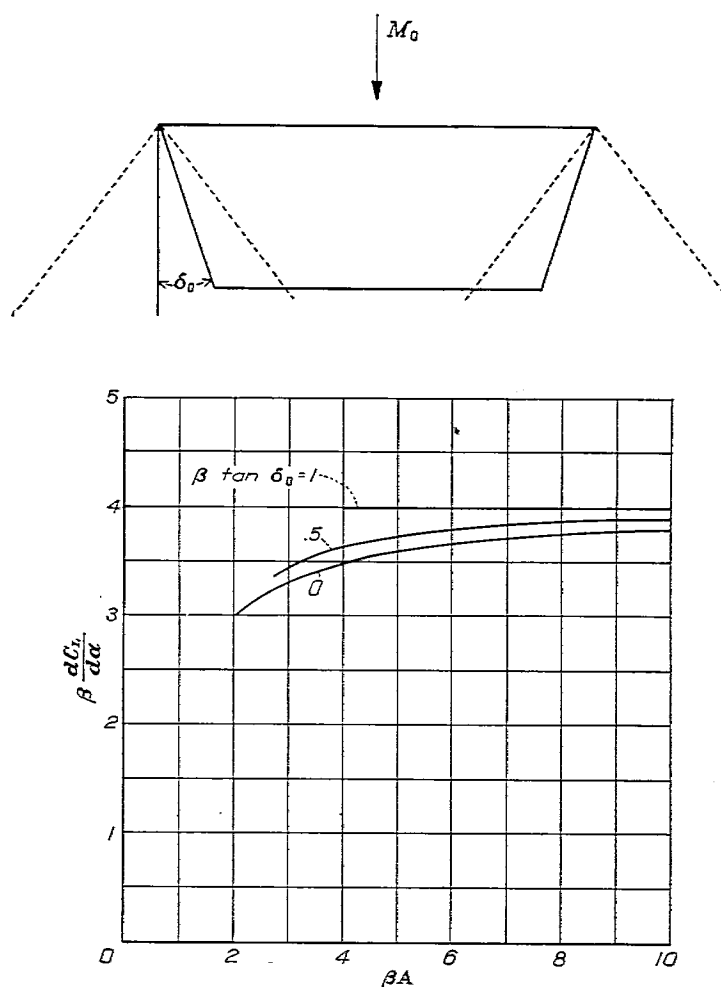


FIGURE 11.—Variation of reduced lift-curve slope  $\beta \frac{dC_L}{d\alpha}$  with reduced aspect ratio  $\beta A$  for various trapezoidal plan forms.

terminated at values of  $A\beta$  for which the tip Mach cones intersect on the trailing edge of the wing.

**Triangular plan form, type 1.**—The pressure distribution over triangular lifting surfaces with constant induced vertical velocities will be developed in the following three sections. These plan forms are indicated in figures 12(a), 12(b), and 12(c) and shall be denoted, respectively, as types 1, 2, and 3. Types 1 and 2 are actually special cases of type 3; namely, the cases where one leading edge is parallel to the free stream, and where both leading edges make equal angles with the stream direction. Type 3 includes any plan form which has leading edges swept behind the Mach cone but on opposite sides of an axis drawn through the vertex of the triangle and parallel to the free stream; and, further, has a trailing edge such that the Mach cones from either tip do not cross the surface of the wing. The principal reason for considering the three types separately is to show the manner in which the spanwise loading appears in the solution of the problem. In types 1 and 2 the proper load distribution is found readily while the final type requires a more careful treatment.

In order to determine the load distribution over the airfoil it will be convenient to use a differential element over which the loading is uniform. The elements may then be summed and the distribution of loading adjusted so that the induced vertical velocity at any point on the total lifting surface is

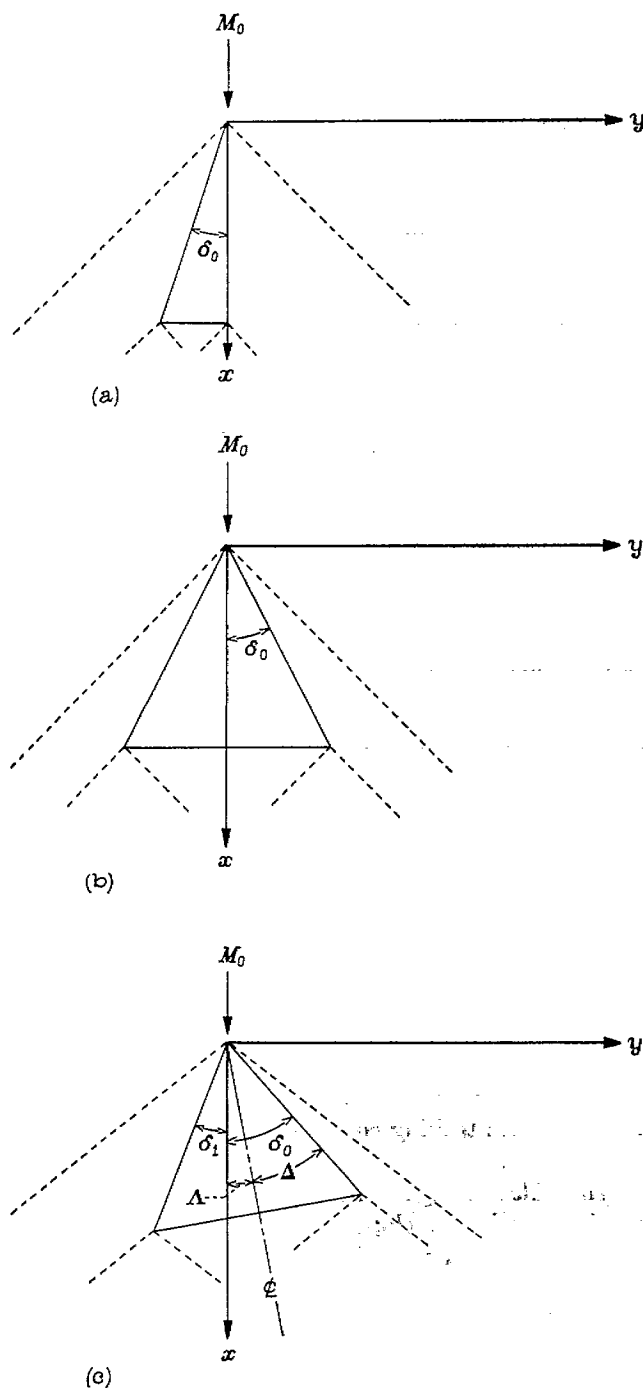


FIGURE 12.—Triangular flat plate lifting surfaces. (a) Type 1. (b) Type 2. (c) Type 3.

constant. For the triangular plan forms it is possible to assume that conical flow exists and the analysis may be carried out using the angular coordinates that have already been introduced.

Figure 13 shows the elemental lifting surface to be used. The sides of the element extend back from the tip of the Mach cone; making angles  $\delta$  and  $\delta + \Delta\delta$  with the positive  $x$  axis or free-stream direction. Corresponding to previous notation, the relations  $\theta = \beta \tan \delta$  and  $\theta + \Delta\theta = \beta \tan (\delta + \Delta\delta)$  are used. The vertical velocity induced by the element of surface may be denoted by  $\Delta w$  and it follows that

$$\Delta w = w(\theta + \Delta\theta, \eta) - w(\theta, \eta)$$

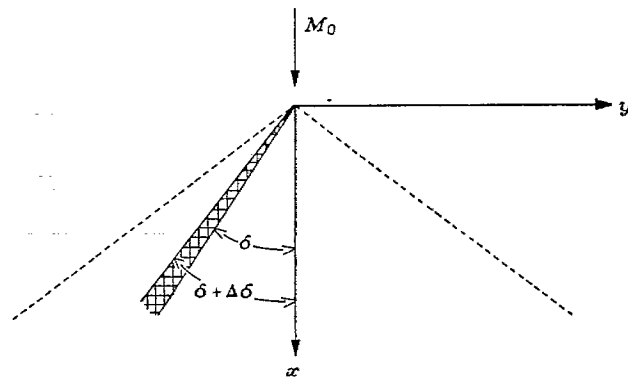


FIGURE 13.—Elemental lifting surface of constant load.

where  $w(\theta, \eta)$  and  $w(\theta + \Delta\theta, \eta)$  are the velocities induced by the triangular-tip surfaces with uniform loading and with tip angles equal to  $\delta$  and  $\delta + \Delta\delta$ , respectively. Applying a limiting process,

$$\lim_{\Delta\theta \rightarrow 0} \frac{\Delta w}{\Delta\theta} = \lim_{\Delta\theta \rightarrow 0} \frac{w(\theta + \Delta\theta, \eta) - w(\theta, \eta)}{\Delta\theta} = \frac{\partial w}{\partial \theta} \quad (60)$$

It follows that  $w_{z=0}$  for the resultant lifting surface will be evaluated by an integration with respect to  $\theta$ . If  $\partial w_{z=0} / \partial \theta$  can be expressed in the form of an integral with respect to  $\eta$ , the relation for  $w_{z=0}$  will then be similar to those given in equations (41) and (52) for the previous plan forms and the expectation will be that the function  $C(\theta)$  can be determined to give constant induced vertical velocity.

The method of attack just outlined is postulated on the existence of an integral expression for  $\partial w_{z=0} / \partial \theta$ . Such an expression is, however, obtainable directly from the integrals in equation (32). Integrating these relations by parts, after first differentiating by  $\theta$ , leads one to the formulas:

For  $-1 < \eta < 0$

$$\frac{\partial w_{z=0}}{\partial \theta} = \frac{\beta C_0}{2\pi V_0} \left[ \frac{\sqrt{1-\eta^2}}{\eta(\eta+\theta)} + \int_{-1}^{\eta} \frac{d\eta_1}{\eta_1^2(\eta_1+\theta)\sqrt{1-\eta_1^2}} \right] \quad (61)$$

and for  $0 < \eta < 1$

$$\frac{\partial w_{z=0}}{\partial \theta} = \frac{\beta C_0}{2\pi V_0} \left[ \frac{\sqrt{1-\eta^2}}{\eta(\eta+\theta)} + \int_1^{\eta} \frac{d\eta_1}{\eta_1^2(\eta_1+\theta)\sqrt{1-\eta_1^2}} \right] \quad (62)$$

If the elements are summed over the type 1 triangular wing, induced vertical velocity is

$$w(\eta)_{z=0} = \frac{\beta}{2\pi V_0} \int_0^{\theta_0} C(\theta) \left[ \frac{\sqrt{1-\eta^2}}{\eta(\eta+\theta)} + \int_{-1}^{\eta} \frac{d\eta_1}{\eta_1^2(\eta_1+\theta)\sqrt{1-\eta_1^2}} \right] d\theta \quad (63)$$

where  $C(\theta) = \varphi_u - \varphi_l$  for the element at  $\delta = \arctan \frac{\theta}{\beta}$ . If  $w_{z=0}$  is constant, then

$$\frac{\partial w_{z=0}}{\partial \eta} = 0$$

and from this criterion the function  $C(\theta)$  will be determined.

Thus, using methods similar to those introduced in the development of equation (42),

$$0 = \frac{\partial}{\partial \eta} \frac{\sqrt{1-\eta^2}}{\eta} \int_0^{\theta_0} \frac{C(\theta)}{\eta+\theta} d\theta + \frac{1}{\eta^2 \sqrt{1-\eta^2}} \int_0^{\theta_0} \frac{C(\theta) d\theta}{\eta+\theta}$$

$$= \frac{\partial}{\partial \eta} \int_0^{\theta_0} \frac{C(\theta) d\theta}{\eta+\theta} \quad (64)$$

The general solution of this equation is

$$C(\theta) = \frac{C_1 \theta + C_2}{\sqrt{\theta(\theta_0 - \theta)}}$$

where  $C_1$  and  $C_2$  are constants. Since, however, the Kutta-Joukowski condition requires that loading vanish along the edge  $\theta=0$ , it follows that  $C_2=0$  and the required loading takes the form

$$C(\theta) = C_1 \sqrt{\frac{\theta}{\theta_0 - \theta}} \quad (65)$$

If equation (65) is substituted into equation (63), vertical induced velocity can be calculated from the expression

$$\frac{2\pi V_0 w_{z=0}}{\beta C_1} = \frac{\sqrt{1-\eta^2}}{\eta} \int_0^{\theta_0} \frac{\theta d\theta}{(\eta+\theta)\sqrt{\theta(\theta_0-\theta)}} + \int_0^{\theta_0} \frac{\theta d\theta}{\sqrt{\theta(\theta_0-\theta)}} \int_{-1}^{\eta} \frac{d\eta_1}{\eta_1^2(\eta_1+\theta)\sqrt{1-\eta_1^2}} \quad (66)$$

The region of integration in the  $\eta_1, \theta$  plane for the double integral of equation (66) is shown in figure 14 for the case in which  $-\theta_0 < \eta < 0$ . A singularity in the integrand of the double integral exists along the line  $\theta + \eta_1 = 0$ . Reversing the order of integration, equation (66) may be rewritten as

$$\frac{2\pi V_0 w_{z=0}}{\beta C_1} = -\sqrt{1-\eta^2} \int_0^{\theta_0} \frac{d\theta}{(\theta+\eta)\sqrt{\theta(\theta_0-\theta)}} - \int_{-1}^{-\theta_0} \frac{d\eta_1}{\eta_1 \sqrt{1-\eta_1^2}} \int_0^{\theta_0} \frac{d\theta}{(\theta+\eta_1)\sqrt{\theta(\theta_0-\theta)}} - \int_{-\theta_0}^{\eta} \frac{d\eta_1}{\eta_1 \sqrt{1-\eta_1^2}} \int_0^{\theta_0} \frac{d\theta}{(\theta+\eta_1)\sqrt{\theta(\theta_0-\theta)}} \quad (67)$$

The single integral in equation (67) has a singularity at  $\theta = -\eta$  since  $-\theta_0 < \eta < 0$  and  $\eta$  therefore lies inside the region

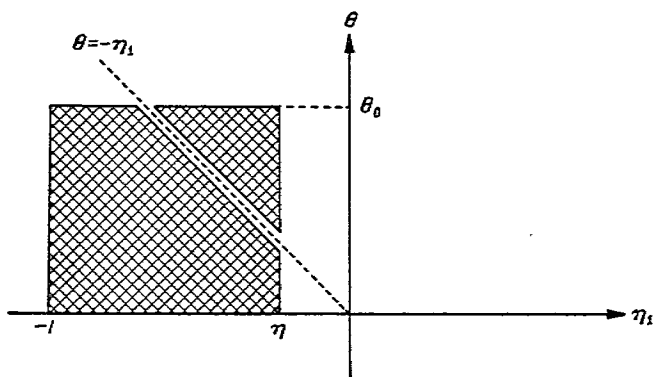


FIGURE 14.—Region of integration showing line of singularity for equations (66) and (78).

of integration. A corresponding singularity occurs in the second of the double integrals at  $\theta = -\eta_1$ . Consider, therefore, the integral

$$\int_0^{\theta_0} \frac{d\theta}{(\theta+\eta)\sqrt{\theta(\theta_0-\theta)}} = \lim_{\epsilon \rightarrow 0} \left[ \int_0^{-\eta-\epsilon} \frac{d\theta}{(\theta+\eta)\sqrt{\theta_0-\theta}} + \int_{-\eta+\epsilon}^{\theta_0} \frac{d\theta}{(\theta+\eta)\sqrt{\theta(\theta_0-\theta)}} \right] \quad (68)$$

The indefinite integral is

$$\frac{1}{\sqrt{-\eta\theta_0-\eta^2}} \ln \frac{-\eta\theta_0 + \theta\theta_0 + 2\eta\theta - 2\sqrt{(-\eta\theta_0-\eta^2)\theta(\theta_0-\theta)}}{\theta+\eta}$$

so that the definite integral is

$$\lim_{\epsilon \rightarrow 0} \frac{1}{\sqrt{-\eta\theta_0-\eta^2}} \left\{ \ln \frac{\theta_0}{-\theta_0} + \ln \frac{[-2\eta\theta_0 - \epsilon\theta_0 - 2\eta^2 - 2\epsilon\eta - 2\sqrt{(-\eta\theta_0-\eta^2)(-\eta-\epsilon)(\theta_0+\eta+\epsilon)}] \epsilon}{[-2\eta\theta_0 + \epsilon\theta_0 - 2\eta^2 + 2\epsilon\eta - 2\sqrt{(-\eta\theta_0-\eta^2)(-\eta+\epsilon)(\theta_0+\eta-\epsilon)}] (-\epsilon)} \right\}$$

The value of this expression is 0 and equation (67) therefore becomes

$$\frac{2\pi V_0 w_{z=0}}{\beta C_1} = - \int_{-1}^{-\theta_0} \frac{d\eta_1}{\eta_1 \sqrt{1-\eta_1^2}} \int_0^{\theta_0} \frac{d\theta}{(\theta+\eta_1)\sqrt{\theta(\theta_0-\theta)}} \quad (69)$$

Since, in this region of integration,  $-1 < \eta < -\theta_0$  it follows that

$$\int_0^{\theta_0} \frac{d\theta}{(\theta+\eta_1)\sqrt{\theta(\theta_0-\theta)}} = \frac{1}{\sqrt{\eta_1\theta_0+\eta_1^2}} \arctan \frac{-\eta_1\theta_0 + \theta\theta_0 + 2\eta_1\theta}{2\sqrt{(\eta_1^2+\eta_1\theta_0)\theta(\theta_0-\theta)}} \Big|_0^{\theta_0} = \frac{-\pi}{\sqrt{\eta_1(\theta_0+\eta_1)}}$$

and

$$w_{z=0} = \frac{\beta C_1}{2V_0} \int_{-1}^{-\theta_0} \frac{d\eta_1}{\eta_1 \sqrt{1-\eta_1^2} \sqrt{\eta_1(\eta_1+\theta_0)}} \quad (70)$$

The integral of equation (70) can be transformed by means of purely algebraic substitutions into a form that integrates immediately into complete elliptic integrals of the first and second kind. However, in the consideration of the type 3 plan form it will be necessary to resort to other methods of transformation, so that a more uniform approach, employing Jacobian elliptic functions, will be used throughout. (See reference 12.)

The quartic under the radical in equation (70) is first reduced to an expression of the type appearing in elliptic integrals of canonical form. This is accomplished by successive application of the transformations

$$\eta_1 = -\frac{k+ls}{1+s} \text{ and } s = \frac{k}{t}$$

where  $k$  and  $l$  are chosen so as to destroy the odd powers of the variable. By means of these transformations, induced velocity becomes

$$w_{z=0} = \frac{\beta C_1}{2V_0} \frac{(1-k^2)k^2}{\sqrt{k(\theta_0-k)(1-k^2)}} \int_1^{\frac{1}{k}} \frac{[t^2 + (k - \frac{1}{k})t - 1]dt}{(1-k^2t^2)\sqrt{(1-t^2)(k^2t^2-1)}} \quad (71)$$

where

$$k = \frac{1 - \sqrt{1 - \theta_0^2}}{\theta_0}$$

The integration of equation (71) will be performed after first considering two parts such that  $w_{z=0} = w_1 + w_2$  where

$$w_1 = \frac{\beta C_1}{2V_0} \frac{(1-k^2)k^2}{\sqrt{k(\theta_0-k)(1-k^2)}} \int_1^{\frac{1}{k}} \frac{(k - \frac{1}{k})tdt}{(1-k^2t^2)\sqrt{(1-t^2)(k^2t^2-1)}}$$

and

$$w_2 = -\frac{\beta C_1}{2V_0} \frac{(1-k^2)k^2}{\sqrt{k(\theta_0-k)(1-k^2)}} \int_1^{\frac{1}{k}} \frac{(1-t^2)dt}{(1-k^2t^2)\sqrt{(1-t^2)(k^2t^2-1)}}$$

This separation is prompted by the fact that the integral for  $w_1$  is expressible in terms of elementary functions after the simple transformation  $t^2 = z$ . The results of such an integration lead to a value that is zero at the lower limit and infinite at the upper limit. However, an inspection of the original integral in equation (70) shows that  $w_{z=0}$  is finite so the infinity obtained for  $w_1$  must be canceled by a corresponding infinity of equal magnitude in  $w_2$ . The actual proof of this statement necessitates, of course, treating the combined expressions as an indeterminate form where the upper limits of the integrals for  $w_1$  and  $w_2$  are replaced by  $\frac{1}{k} + \epsilon$  and the limit is taken as  $\epsilon$  approaches zero.

Introduce now in the integration of  $w_2$  Jacobian elliptic functions and set

$$t = sn(u, k) = snu$$

so that

$$dt = cnu \, dnu \, du$$

The expression for  $w_2$  becomes

$$w_2 = \frac{\beta C_1}{2V_0} \frac{(1-k^2)k^2}{\sqrt{k(\theta_0-k)(1-k^2)}} \int_K^{K+ik'} \frac{cn^2u}{dn^2u} du$$

where  $K$  and  $K'$  are the complete elliptic integrals of the first kind with respective moduli  $k$  and  $k' = \sqrt{1-k^2}$ . Integrating and combining with  $w_1$ , one has

$$w_{z=0} = w_1 +$$

$$\frac{\beta C_1}{2V_0} \frac{(1-k^2)k^2}{\sqrt{k(\theta_0-k)(1-k^2)}} \left\{ \frac{1}{k^2} \left[ u + k^2 \frac{snu \, cnu}{dnu} - E(u) \right] \right\}_K^{K+ik'}$$

where  $E(u)$  is the incomplete elliptic integral of the second kind. After substitution of the limits, induced vertical velocity is

$$w_{z=0} = -\frac{\beta C_1}{2V_0} \frac{(1-k^2)E'}{\sqrt{k(\theta_0-k)(1-k^2)}} \quad (72)$$

where  $E'$  is the complete elliptic integral of the second kind with modulus  $k' = \sqrt{1-k^2}$ . Equation (72) can be further simplified by writing  $k$  in terms of  $\theta_0$  so that

$$w_{z=0} = -\frac{\beta C_1}{2V_0} \sqrt{\frac{2(1+\sqrt{1-\theta_0^2})}{\theta_0^2}} E' \quad (73)$$

where the modulus of  $E'$  is  $\sqrt{1-k^2}$  and  $k = \frac{1 - \sqrt{1 - \theta_0^2}}{\theta_0}$

For the loading in question

$$p_i - p_u = \rho_0(\varphi_u - \varphi_i) = \rho_0 C_1 \sqrt{\frac{\theta}{\theta_0 - \theta}}$$

and

$$\frac{p_i - p_u}{\frac{1}{2} \rho_0 V_0^2} = \frac{\Delta p}{q} = \frac{2C_1}{V_0^2} \sqrt{\frac{\theta}{\theta_0 - \theta}}$$

By means of equation (73) the constant  $C_1$  may be eliminated and

$$\frac{\Delta p}{q} = \frac{2\alpha}{\beta E'} \sqrt{\frac{2\theta(1 - \sqrt{1 - \theta_0^2})}{\theta_0 - \theta}} \quad (74)$$

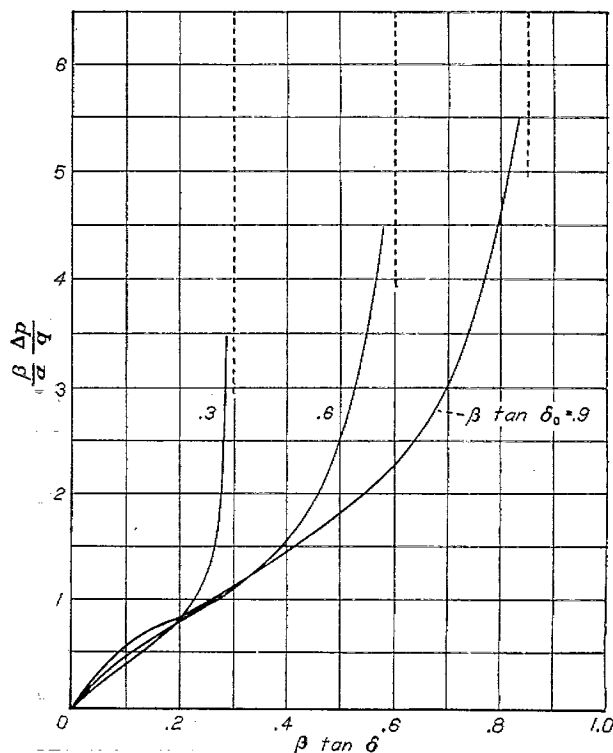
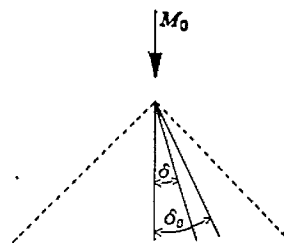


FIGURE 15.—Load distribution over triangular plan forms of type 1.



Figure 15 shows the variation of  $\frac{\beta}{\alpha} \frac{\Delta p}{q}$  with  $\beta \tan \delta$  for values of  $\beta \tan \delta_0$  equal to 0.3, 0.6, and 0.9.

From equations (74) and (49) the lift coefficient of the right triangle wing with trailing edge normal to the free-stream direction can be determined. It follows that

$$C_L = \frac{\pi \alpha}{\beta E'} \sqrt{2(1 - \sqrt{1 - \theta_0^2})} \quad (75)$$

Since the aspect ratio  $A$  is given by the equation  $A = 2\theta_0/\beta$ , equation (75) can be used to find the lift-curve slope as a function of  $A$ . In figure 16 a plot of  $\beta \frac{dC_L}{d\alpha}$  as a function of  $\beta A$  is given.

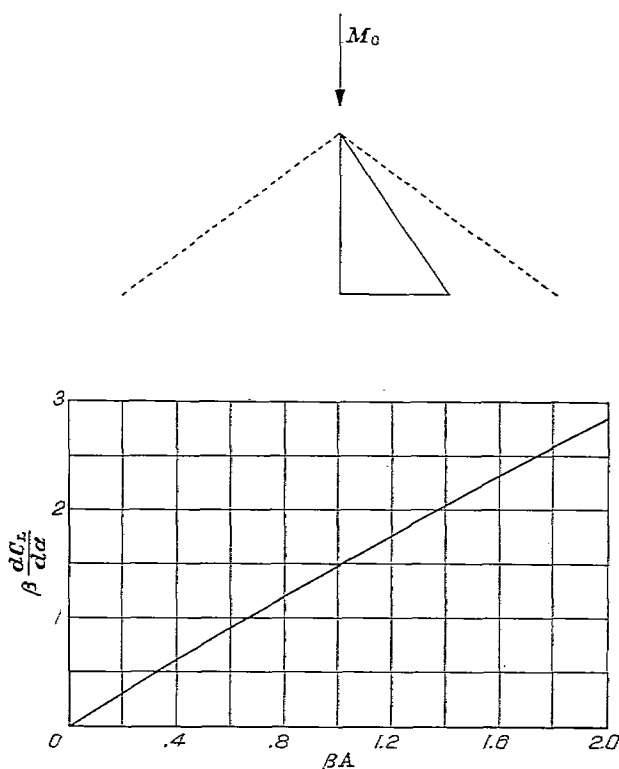


FIGURE 16.—Variation of reduced lift-curve slope  $\beta \frac{dC_L}{d\alpha}$  with reduced aspect ratio  $\beta A$  for plan forms of type 1.

**Triangular plan form, type 2.**—Figure 12(b) shows the symmetrical type of triangular plan form considered in this section. The semivertex angle is  $\delta_0$  and  $\theta_0$  is defined by the relation

$$\theta_0 = \beta \tan \delta_0$$

The loading element used in the previous section can be used again and equations (61) and (62) are applicable directly. Because of the symmetry of the figure, it is necessary merely to insure the constancy of  $w_{z=0}$  over the left half of the wing in order that the entire wing be a flat plate.

Summing the elements over the type 2 triangular wing, induced vertical velocity over the portion of the wing for which  $-1 < \eta < 0$  is

$$w(\eta)_{z=0} = \frac{\beta}{2\pi V_0} \int_{-\theta_0}^{\theta_0} \left[ \frac{\sqrt{1-\eta^2}}{\eta(\eta+\theta)} + \int_{-1}^{\eta} \frac{d\eta_1}{\eta_1^2(\eta_1+\theta)\sqrt{1-\eta_1^2}} \right] C(\theta) d\theta$$

or, since  $C(\theta) = C(-\theta)$ ,

$$w(\eta)_{z=0} = -\frac{\beta}{\pi V_0} \int_0^{\theta_0} \left[ \frac{\sqrt{1-\eta^2}}{\theta^2-\eta^2} + \int_{-1}^{\eta} \frac{d\eta_1}{\eta_1(\theta^2-\eta_1^2)\sqrt{1-\eta_1^2}} \right] C(\theta) d\theta \quad (76)$$

The function  $C(\theta)$  in equation (76) must give a constant value for  $w(\eta)_{z=0}$  so that  $\partial w_{z=0}/\partial \eta$  will vanish. Imposing this condition it can be shown that a solution is given by the relation

$$C(\theta) = \frac{C_1}{\sqrt{\theta_0^2 - \theta^2}} \quad (77)$$

and, after substitution in equation (76),

$$\frac{\pi V_0 w_{z=0}}{\beta C_1} = - \int_0^{\theta_0} \frac{\sqrt{1-\eta^2} d\theta}{(\theta^2-\eta^2)\sqrt{\theta_0^2-\theta^2}} - \int_0^{\theta_0} \frac{d\theta}{\sqrt{\theta_0^2-\theta^2}} \int_{-1}^{\eta} \frac{d\eta_1}{\eta_1 \sqrt{1-\eta_1^2}(\theta^2-\eta_1^2)} \quad (78)$$

The integration of equation (78) is to be performed under the assumption that  $-\theta_0 < \eta < 0$  so that the region of integration in the  $\eta_1, \theta$  plane for the double integral is as shown in figure 14. Reversing the order of integration in the double integral, equation (78) may be written in the form

$$\frac{\pi V_0 w_{z=0}}{\beta C_1} = - \int_0^{\theta_0} \frac{\sqrt{1-\eta^2} d\theta}{(\theta^2-\eta^2)\sqrt{\theta_0^2-\theta^2}} - \int_{-1}^{-\theta_0} \frac{d\eta_1}{\eta_1 \sqrt{1-\eta_1^2}} \int_0^{\theta_0} \frac{d\theta}{(\theta^2-\eta_1^2)\sqrt{\theta_0^2-\theta^2}} - \int_{-\theta_0}^{\eta} \frac{d\eta_1}{\eta_1 \sqrt{1-\eta_1^2}} \int_0^{\theta_0} \frac{d\theta}{(\theta^2-\eta_1^2)\sqrt{\theta_0^2-\theta^2}} \quad (79)$$

Evaluation of integrals of the form

$$I = - \int_0^{\theta_0} \frac{d\theta}{(\theta^2-\eta^2)\sqrt{\theta_0^2-\theta^2}}$$

is accomplished by means of the substitution

$$x = \frac{\theta}{\theta_0}$$

After substitution, the integral becomes

$$I = \frac{1}{\theta_0^2} \int_0^1 \frac{dx}{\left( \frac{\eta^2}{\theta_0^2} - x^2 \right) \sqrt{1-x^2}}$$

and, by straightforward integration,

$$I = \begin{cases} 0 & \text{for } \frac{\eta^2}{\theta_0^2} < 1 \\ \frac{\pi}{2\eta\sqrt{\eta^2-\theta_0^2}} & \text{for } \frac{\eta^2}{\theta_0^2} > 1 \end{cases}$$

This result shows that the second double integral of equation (79) vanishes (since  $\theta_0^2 > \eta_1^2$ ) as does also the single integral in the equation. For the remaining double integral, however,  $\theta_0^2 < \eta_1^2$  and

$$w_{z=0} = \frac{\beta C_1}{2V_0} \int_{-1}^{-\theta_0} \frac{d\eta_1}{\eta_1^2 \sqrt{1-\eta_1^2} \sqrt{\eta_1^2 - \theta_0^2}} \quad (80)$$

Setting

$$z = -\frac{1}{\eta_1}$$

equation (71) transforms to

$$w_{z=0} = -\frac{\beta C_1}{2V_0} \int_1^{\frac{1}{\theta_0}} \frac{z^2 dz}{\sqrt{(z^2-1)(1-\theta_0^2 z^2)}}$$

Introducing the modulus  $k = \theta_0$  and making the substitution

$$z = sn(u, k) = snu$$

one gets the expression

$$\begin{aligned} w_{z=0} &= \frac{i\beta C_1}{2V_0} \int_K^{K+iK'} sn^2 u du \\ &= \frac{i\beta C_1}{2V_0 k^2} [u - E(u)]_K^{K+iK'} \\ &= -\frac{\beta C_1}{2V_0 k^2} E' \end{aligned}$$

where the prime again refers to the complementary modulus  $k' = \sqrt{1-k^2}$  of the complete elliptic integral. Since  $k = \theta_0$

$$w_{z=0} = -\frac{\beta C_1}{2V_0 \theta_0^2} E' \quad (81)$$

where  $k' = \sqrt{1-\theta_0^2}$

For the loading in question

$$\frac{p_l - p_u}{\frac{1}{2} \rho_0 V_0^2} = \frac{\Delta p}{q} = \frac{2C_1}{V_0^2 \sqrt{\theta_0^2 - \theta^2}}$$

so that, eliminating  $C_1$  between this equation and equation (81),

$$\frac{\Delta p}{q} = \frac{4\alpha \theta_0^2}{\beta \sqrt{\theta_0^2 - \theta^2} E'} \quad (82)$$

Figure 17 shows the variation of  $\frac{\beta \Delta p}{\alpha q}$  with  $\beta \tan \delta$  for values of  $\beta \tan \delta_0$  equal to 0.3, 0.6, and 0.9.

From equations (82) and (49) it is possible to find the expression for lift coefficient of a triangular or delta wing. Thus:

$$C_L = \frac{2\pi \theta_0 \alpha}{\beta E'} \quad (83)$$

Since aspect ratio of the wing is

$$A = \frac{4\theta_0}{\beta}$$

lift coefficient becomes

$$C_L = \frac{\pi \alpha A}{2E'} \quad (84)$$

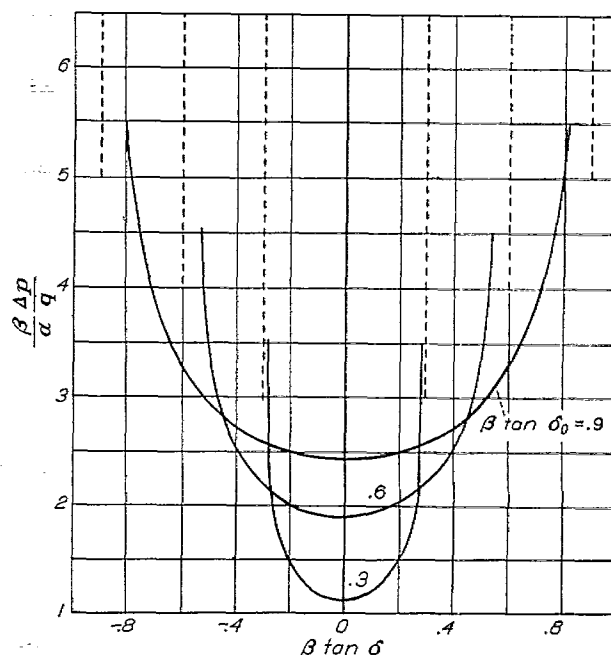
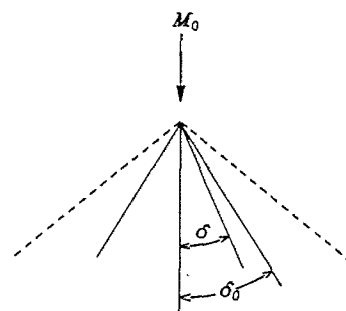


FIGURE 17.—Load distribution over triangular plan forms of type 2.

where the modulus of  $E'$  is  $k' = \sqrt{1 - \frac{A^2 \beta^2}{16}}$ . This result agrees with that obtained in another manner by Stewart (reference 8). In figure 18 a plot is given of  $\beta \frac{dC_L}{d\alpha}$  as a function of  $\beta A$ .

**Triangular plan form, type 3.**—Figure 12 (c) shows the plan form now to be considered. Relative to the  $x$  axis or free-stream direction the sides of the triangle form the angles  $\delta_0$  and  $\delta_1$  so that the total vertex angle is  $\delta_0 + \delta_1 = 2\Delta$ . The variables  $\theta_0$  and  $\theta_1$  are also introduced satisfying the relations  $\theta_0 = \beta \tan \delta_0$ ,  $\theta_1 = \beta \tan \delta_1$ . The same loading element that was used for type 1 and type 2 triangles may be used and equations (61) and (62) apply. It will then be necessary to determine the distribution of load so that the induced vertical velocity over the plan form is a constant. Since this induced velocity must be the same on both sides of the  $\delta = 0$  axis, two equations result:

For  $-1 < \eta < 0$

$$w(\eta)_{z=0} = \frac{\beta}{2\pi V_0} \int_{-\theta_1}^{\theta_0} \left[ \frac{\sqrt{1-\eta^2}}{\eta(\eta+\theta)} + \int_{-1}^{\eta} \frac{d\eta_1}{\eta_1^2(\eta_1+\theta)\sqrt{1-\eta_1^2}} \right] C(\theta) d\theta \quad (85)$$

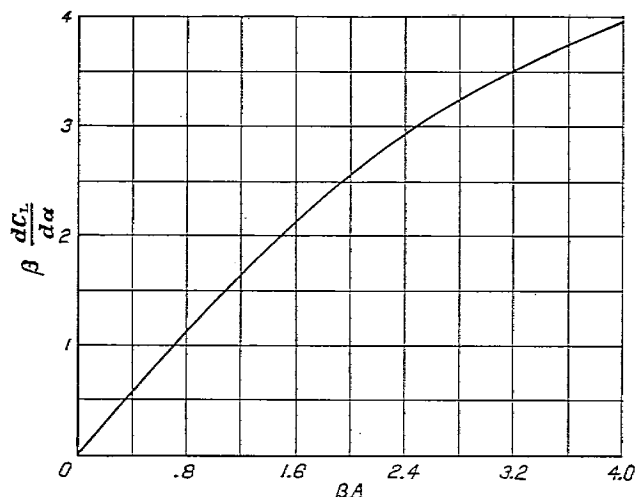
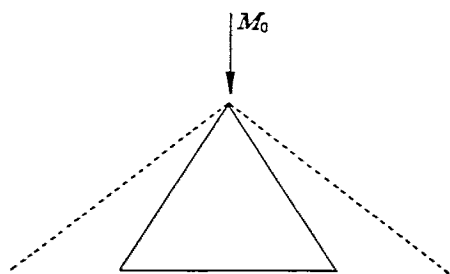


FIGURE 18.—Variation of reduced lift-curve slope  $\beta \frac{dC_L}{d\alpha}$  with reduced aspect ratio  $\beta A$  for plan forms of type 2.

and for  $0 < \eta < 1$

$$w(\eta)_{z=0} = \frac{\beta}{2\pi V_0} \int_{-\theta_1}^{\theta_1} \left[ \frac{\sqrt{1-\eta^2}}{\eta(\eta+\theta)} + \int_1^\eta \frac{d\eta_1}{\eta_1^2(\eta_1+\theta)\sqrt{1-\eta_1^2}} \right] C(\theta) d\theta \quad (86)$$

From the solutions to the problems of type 1 and type 2 it is possible to construct a solution of the more general problem by expressing the loading function in the form

$$C(\theta) = \frac{A\theta + B}{\sqrt{(\theta_1 + \theta)(\theta_0 - \theta)}} \quad (87)$$

where  $A$  and  $B$  are constants that can be determined in terms of  $w_{z=0}$  from equations (85) and (86). Equation (87), in conjunction with equations (85) and (86), yields the expressions

$$\begin{aligned} w_{z=0} &= \frac{\beta}{2V_0} [AH_1(\theta_0, \theta_1) + BH_2(\theta_0, \theta_1)] \\ w_{z=0} &= \frac{\beta}{2V_0} [-AH_1(\theta_1, \theta_0) + BH_2(\theta_1, \theta_0)] \end{aligned} \quad (88)$$

where

$$H_1(\theta_1, \theta_0) = \int_1^{\theta_1} \frac{d\eta_1}{\eta_1 \sqrt{(1-\eta_1^2)(\eta_1 - \theta_1)(\eta_1 + \theta_0)}} \quad (89)$$

$$H_2(\theta_1, \theta_0) = \int_1^{\theta_1} \frac{d\eta_1}{\eta_1^2 \sqrt{(1-\eta_1^2)(\eta_1 - \theta_1)(\eta_1 + \theta_0)}} \quad (90)$$

The evaluation of  $H_1(\theta_1, \theta_0)$  and  $H_2(\theta_1, \theta_0)$  is accomplished in the same manner as has been used previously: first, a reduction of the quartic under the radical to canonical form and second, transformation by means of Jacobian elliptic functions followed by direct integration. Since the calculations for both equations are quite similar, only in the case of  $H_1(\theta_1, \theta_0)$  will the details be mentioned.

By means of the transformations  $\eta_1 = \frac{a+bs}{1+s}$  and  $s = \frac{a}{t}$ , where

$$a = \frac{1 - \theta_0\theta_1 - \sqrt{(1-\theta_0^2)(1-\theta_1^2)}}{\theta_0 - \theta_1} \quad (91)$$

$$b = \frac{1 - \theta_0\theta_1 + \sqrt{(1-\theta_0^2)(1-\theta_1^2)}}{\theta_0 - \theta_1} \quad (92)$$

The introduction of the symbols  $R$  and  $k$  defined as

$$R = \frac{b-a}{\sqrt{(1-a^2)(\theta_0-a)(\theta_1+a)}} \quad (93)$$

$$k = \frac{1+\theta_0b}{\theta_0+b} \quad (94)$$

equation (89) reduces to

$$H_1 = a^2 R k \int_1^{\frac{1}{k}} \frac{[t^2 + t(a-b) - 1] dt}{(1-a^2t^2)\sqrt{(t^2-1)(1-k^2t^2)}} \quad (95)$$

The integrand divides naturally into two parts, one containing even powers and one containing odd powers of  $t$  in the numerator. The latter part integrates into elementary functions after substituting  $t = u^2$  and equation (95) thereby becomes

$$H_1 = a^2 R k \left[ -\frac{\pi}{2} \sqrt{\frac{b^2-1}{k^2-a^2}} + \int_1^{\frac{1}{k}} \frac{(t^2-1) dt}{(1-a^2t^2)\sqrt{(t^2-1)(1-k^2t^2)}} \right] \quad (96)$$

Setting

$$I_2 = \int_1^{\frac{1}{k}} \frac{(t^2-1) dt}{(1-a^2t^2)\sqrt{(t^2-1)(1-k^2t^2)}}$$

and substituting

$$x = sn(u, k) = snu$$

one gets

$$I_2 = i \int_K^{K+iK'} \left[ 1 + (a^2-1) \frac{sn^2u}{1-a^2sn^2u} \right] du$$

If  $sn \gamma = \frac{a}{k}$ ,  $I_2$  now may be written as

$$I_2 = -K' - i \int_K^{K+iK'} \frac{dn\gamma}{k^2 sn\gamma cn\gamma} \frac{k^2 sn\gamma cn\gamma dn\gamma sn^2u}{1-k^2 sn^2\gamma sn^2u} du$$

or

$$I_2 = -K' - i \sqrt{\frac{b^2-1}{k^2-a^2}} [\Pi(u, \gamma)]_K^{K+iK'} \quad (97)$$

where  $\Pi(u, \gamma)$  is the fundamental elliptic integral of the third kind.

The evaluation of  $\Pi(u, k)$  is best achieved by means of its expression in terms of theta functions and zeta functions. Thus

$$\Pi(u, \gamma) = \frac{1}{2} \log \frac{\theta(u - \gamma)}{\theta(u + \gamma)} + uZ(\gamma)$$

and the bracketed term in equation (88) is

$$\Pi(K + iK', \gamma) - \Pi(K, \gamma) = \frac{1}{2} \log \frac{\theta(K + iK' - \gamma)\theta(K + \gamma)}{\theta(K - \gamma)\theta(K + iK' + \gamma)} + iK'Z(\gamma)$$

The theta functions are quasi-periodic, that is, they satisfy the relations

$$\theta(u + 2K) = \theta(u)$$

$$\theta(u + 2iK') = -e^{\frac{\pi}{K}(K' - iu)} \theta(u)$$

From this property, together with the fact that  $\theta(u)$  is an even function, it follows that

$$\frac{\theta(K + iK' - \gamma)\theta(K + \gamma)}{\theta(K - \gamma)\theta(K + iK' + \gamma)} = e^{\frac{i\pi\gamma}{K}}$$

Moreover, since

$$Z(\gamma) = E(\gamma) - \gamma \frac{E}{K}$$

there results

$$\Pi(K + iK', \gamma) - \Pi(K, \gamma) = iK'E(\gamma) - i\gamma \frac{K'E}{K} + i \frac{\pi\gamma}{2K}$$

and

$$I_2 = -K' + \sqrt{\frac{b^2 - 1}{k^2 - a^2}} \left\{ \frac{\pi\gamma}{2K} + K' \left[ E(\gamma) - \gamma \frac{E}{K} \right] \right\} \quad (98)$$

The expression for equation (96) can now be written

$$H_1 = a^2 Rk \sqrt{\frac{b^2 - 1}{k^2 - a^2}} \left\{ \frac{\pi}{2} \left[ \frac{\gamma}{K} - 1 \right] + K' \left[ E(\gamma) - \gamma \frac{E}{K} \right] \right\} - a^2 RkK' \quad (99)$$

where the moduli are  $k$  for the nonprimed functions and  $k' = \sqrt{1 - k^2}$  for the primed functions. By definition,  $\gamma = \text{arc sn } \frac{a}{k} = F\left(\frac{a}{k}, k\right)$  where  $F$  is the incomplete elliptic integral of the first kind with argument  $\frac{a}{k}$  and modulus  $k$ .

In the same notation, the equation for  $H_2$  is as follows:

$$H_2 = \frac{kRb}{b^2 k^2 - 1} \left\{ a^2(1 - k^2)K' - (1 - a^2)E' - a(1 - k^2) \sqrt{\frac{b^2 - 1}{b^2 k^2 - 1}} \left[ K' E(\gamma) - \gamma \frac{EK'}{K} + \frac{\pi}{2} \left( \frac{\gamma}{K} - 1 \right) \right] \right\} \quad (100)$$

Formulas (99) and (100) can now be combined with equations (79) to give

$$A = -\frac{V_0 w_{z=0}}{\beta E'} (\theta_0 - \theta_1) \sqrt{\frac{2G}{\theta_0 + \theta_1}} \quad (101)$$

and

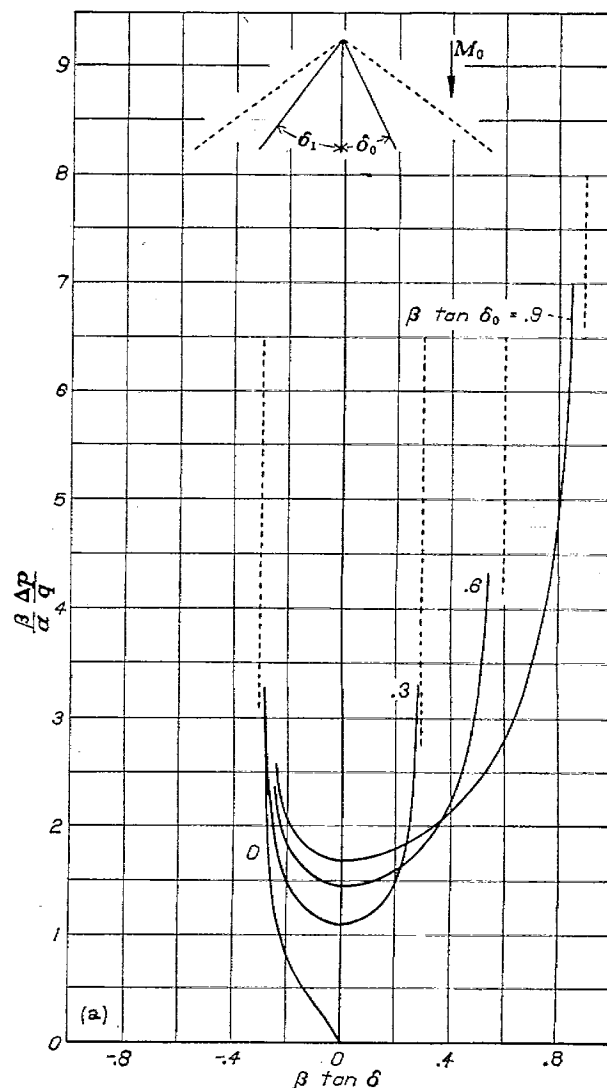


FIGURE 19.—Load distribution over triangular plan forms of type 3. (a)  $\beta \tan \delta_1 = 0.3$ .

$$B = -\frac{V_0 w_{z=0}}{\beta E'} 2\theta_0 \theta_1 \sqrt{\frac{2G}{\theta_0 + \theta_1}} \quad (102)$$

where

$$G = \frac{1 + \theta_0 \theta_1 - \sqrt{(1 - \theta_0^2)(1 - \theta_1^2)}}{\theta_0 + \theta_1} \quad (103)$$

and  $E'$  is the complete elliptic integral of the second kind with modulus  $\sqrt{1 - G^2}$ .

From equations (87), (101), and (102)

$$\begin{aligned} \frac{p_t - p_u}{\frac{1}{2} \rho_0 V_0^2} &= \frac{\Delta p}{q} = \frac{2C(\theta)}{V_0^2} = \frac{2}{V_0^2} \frac{A\theta + B}{\sqrt{(\theta_1 + \theta)(\theta_0 - \theta)}} \\ &= \frac{2\alpha}{\beta E'} \sqrt{\frac{2G}{\theta_0 + \theta_1}} \left[ \frac{(\theta_0 - \theta_1)\theta + 2\theta_0\theta_1}{\sqrt{(\theta_1 + \theta)(\theta_0 - \theta)}} \right] \end{aligned} \quad (104)$$

It should be remarked that the slope of the loading curve is zero at  $\theta = 0$ . Figures 19 (a), 19 (b), and 19 (c) show the variation of  $\frac{\beta \Delta p}{\alpha q}$  with  $\beta \tan \delta$  for values of  $\beta \tan \delta_1$  equal to 0.3, 0.6, and 0.9, respectively, and for  $\beta \tan \delta_0$  equal to 0, 0.3, 0.6, and 0.9.



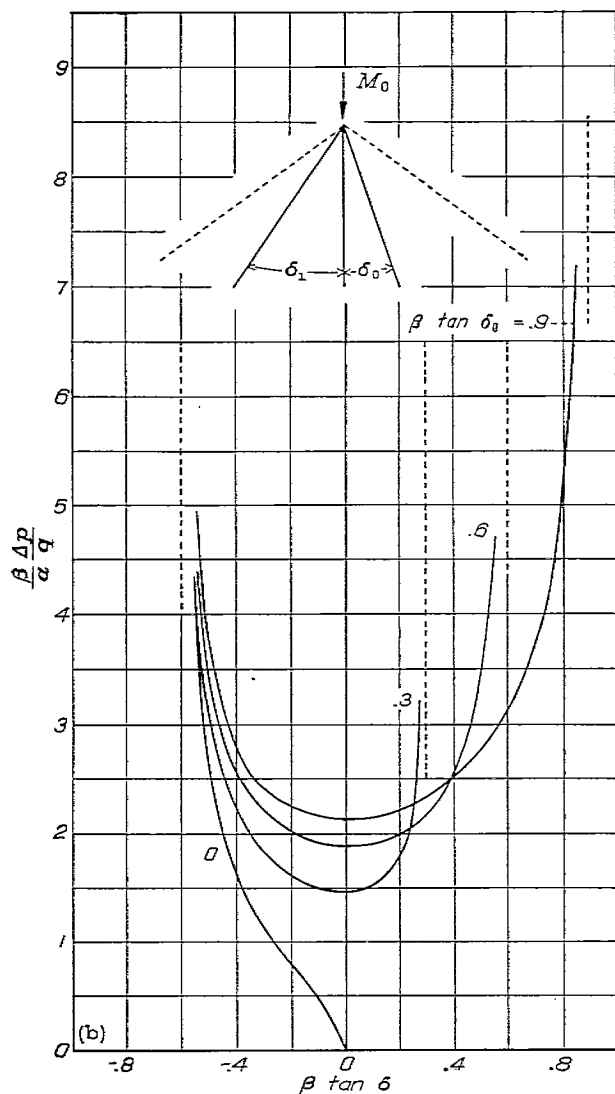


FIGURE 19.—Continued. (b)  $\beta \tan \delta_1 = 0.6$ .

From equations (49) and (104) the lift coefficient for a type 3 plan form is obtainable. Two cases will be developed here: first, when the trailing edge of the wing is perpendicular to the stream direction; second, when the trailing edge of the wing is perpendicular to the line of symmetry. The first configuration may be referred to as a skewed wing while the second configuration may be referred to as a symmetrical delta wing at an angle of sideslip. Thus for a skewed wing

$$C_L = \frac{\pi \alpha}{E' \beta} \sqrt{(\theta_0 + \theta_1) 2G} \quad (105)$$

where  $G$  is given by equation (103) and  $E'$  has the modulus  $\sqrt{1-G^2}$ . This result agrees with that given by R. C. Roberts in an abstract in reference 13.

For the more practical case of the delta wing at an angle of sideslip, figure 12 (c), the lift coefficient can be expressed as

$$C_L = \frac{2\alpha\pi}{E'} \cos \Delta \sqrt{\frac{G \tan \Delta}{\beta}} \quad (106)$$

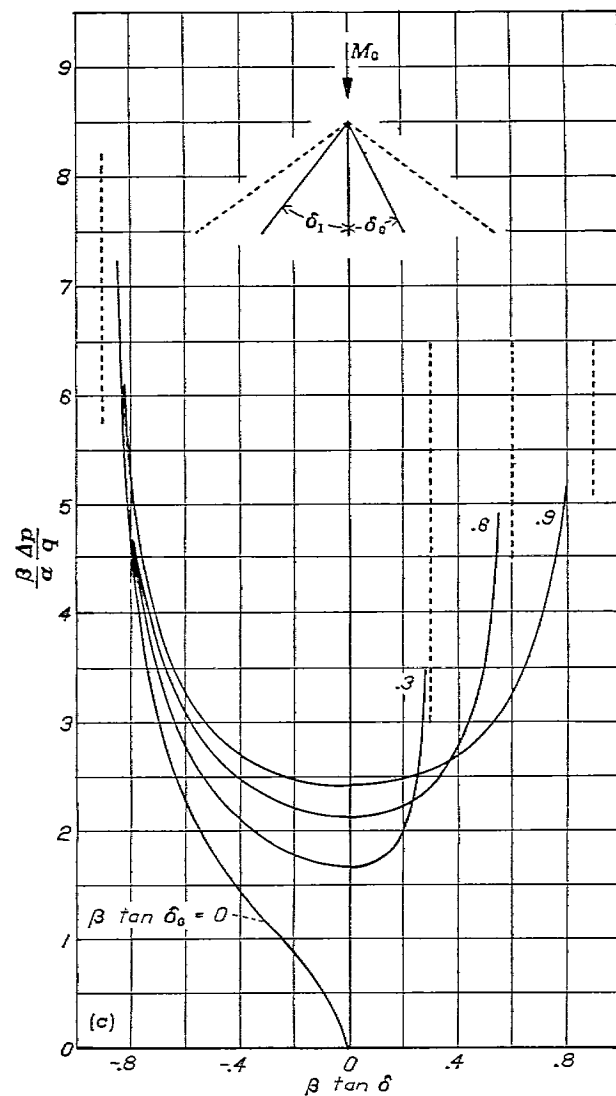


FIGURE 19.—Concluded. (c)  $\beta \tan \delta_1 = 0.9$ .

where  $\Delta$  is the angle of sideslip and  $2\Delta$  the angle between the leading edges, and  $G$  is expressed in terms of  $\theta_0$  and  $\theta_1$  which are, in turn, expressed in terms of  $\Delta$  and  $\Delta$  by the following equations

$$\left. \begin{aligned} \theta_0 &= \beta \tan (\Delta + \Delta) \\ \theta_1 &= \beta \tan (\Delta - \Delta) \end{aligned} \right\} \quad (107)$$

Since the pressure distribution has been computed only for wings with leading edges behind the Mach cone springing from the apex and with a trailing edge ahead of the Mach cones from the wing tips, formula (106) is valid only for cases where

$$\left. \begin{aligned} \mu + \Delta &< 90^\circ \\ \Delta + \Delta &< \mu \\ \Delta - \Delta &> 0 \end{aligned} \right\} \quad (108)$$

These restrictions are practically always met, however, for angles of sideslip likely to be encountered in flight.

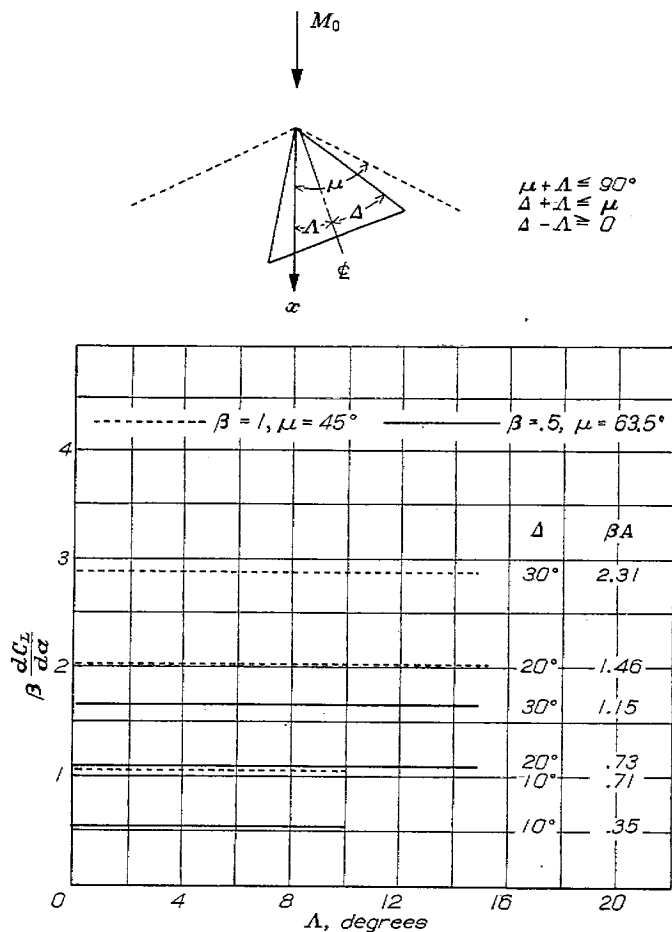


FIGURE 20.—Variation of reduced lift-curve slope  $\beta \frac{dC_L}{d\alpha}$  with angle of sideslip  $\Delta$  for some plan forms of type 3.

Equation (106) is plotted in figure 20 where  $\beta \frac{dC_L}{d\alpha}$  is

shown as a function of sideslip and  $\Delta$ . The figure shows that up to  $15^\circ$  of sideslip  $\beta \frac{dC_L}{d\alpha}$  remains practically constant.

AMES AERONAUTICAL LABORATORY,  
 NATIONAL ADVISORY COMMITTEE FOR AERONAUTICS,  
 MOFFETT FIELD, CALIF., April 14, 1947.

#### REFERENCES

1. Prandtl, L.: General Considerations on the Flow of Compressible Fluids. NACA TM No. 805, 1936.
2. Prandtl, L.: Theorie der flugzeugtragflügel in zusammendrückbaren medium. Luftfahrtforschung, Bd. 13, Oct. 1936.
3. Bateman, H.: Partial Differential Equations of Mathematical Physics. Dover Publications (New York), 1944.
4. Webster, Arthur Gordon: Partial Differential Equations of Mathematical Physics. G. E. Stechert & Co. (New York), 1933.
5. Hadamard, J.: Lectures on Cauchy's Problem in Linear Partial Differential Equations. Yale University Press, 1928.
6. Lamb, Horace: Hydrodynamics. Dover Publications (New York), 1945.
7. Buseman, A.: Infinitesimal Conical Supersonic Flow. NACA TM No. 1100, 1947.
8. Stewart, H. J.: The Lift of a Delta Wing at Supersonic Speeds. Quarterly of Applied Mathematics, Vol. IV, No. 3, Oct. 1946, pp. 246-254.
9. Lagerstrom, P. A.: The Application of Analytic Extension in the Solution of Problems in Supersonic Conical Flows. Abst. No. 7, pub. No. 3, JPL, GALCIT, 1946.
10. Ackert, J.: Air Forces on Airfoils Moving Faster than Sound. NACA TM No. 317, 1925.
11. Schlichting, H.: Airfoil Theory at Supersonic Speed. NACA TM No. 897, 1939.
12. Whittaker, E. T., and Watson, G. N.: A Course of Modern Analysis. 4th Edition, Cambridge University Press, 1940.
13. Roberts, R. C.: On the Lift of a Triangular Wing at Supersonic Speeds. Abst. No. 382, Bulletin of the American Mathematical Society, Vol. 52, No. 11, pt. 1, Nov. 1946.